ABSTRACT

DENG, YU. Flexible and Stretchable Piezoresistive Composites for Strain Sensors. (Under the direction of Dr. Jingyan Dong).

The demand for flexible and stretchable strain sensors has been steadily increasing due to the rapid development of emerging industries such as health monitoring, motion detection, entertainment and robot control. The outstanding deformability and easy fabrication distinguish a flexible and stretchable strain sensor from its counterparts and various experiments have been done to further improve its piezoresistive performance and mechanical properties. Approaches taken can be roughly categorized into three types: new conductive filler, new polymer matrix and new fabrication method.

This research is devoted to exploring relations between the conductive fillers and the polymer matrix of the piezoresistive composite (including metal material and carbon material) and introducing a cost-efficient fabrication method for flexible and stretchable strain sensors with high sensitivity. Piezoresistive performance results of the produced composites are analyzed and compared with market-available commercial piezoresistive product. Our strain sensors, including 83% Nickel-PDMS composite and 35% Graphite-PDMS composite, can achieve good sensitivity at a low compressive strain (<10%) with a gauge factor of 10 and at a high compressive strain (up to 28%) with a gauge factor of 100. Additionally, by simplifying the fabrication processes, the fabrication procedures are shortened and potential application in industries are broadened.

Flexible and Stretchable Piezoresistive Composites for Strain Sensors

by
Yu Deng

A thesis submitted to the Graduate Faculty of
North Carolina State University
in partial fulfillment of the
requirements for the degree of
Master of Science

Industrial Engineering

Raleigh, North Carolina
2020

APPROVED BY

_____	_____
Dr. Jingyan Dong Committee Chair	Dr. Reha Uzsoy
_____	
Dr. Karen Chen	

BIOGRAPHY

Yu Deng was born and raised in Nanjing, Jiangsu, China in 1996. He received his bachelor's degree in mechanical engineering in Shanghai University in June 2018. He attended the Department of Industrial and Systems Engineering, North Carolina State University as a Master of Science Student in August 2018. After the first semester, he joined the research group of Dr. Jingyan Dong and has been working on the piezoresistive composites ever since.

ACKNOWLEDGMENTS

I would like to express my deepest gratitude to my advisor Dr. Jingyan Dong for giving me this opportunity to join the team and complete the research. He has always been willing to giving me guidance and encouragement. His suggestion and advice on my thesis were crucial for the accomplishment of study. Also, I would have my thanks to Dr. Karen Chen and Dr. Reha Uzsoy for being my committee members and responsible for my study.

I would like to extend my sincere appreciation to those who helped me during the time, including my fellow lab mates Yang Cao and Pin Ren, for solving the questions I met with patience and my roommates who accompanied me all the time.

Finally, I would like to thank my family who always be there for me with loving considerations and understanding throughout the years. This work would have been impossible without all your help.

TABLE OF CONTENTS

LIST OF TABLES v
LIST OF FIGURES vi

CHAPTER 1 INTRODUCTION 1
1.1 Introduction 1
1.2 Motivation and Objectives 3
CHAPTER 2 LITERATURE REVIEW 5
2.1 Conductive Filler 5
2.1.1 Graphite 5
2.1.2 Nickel 9
2.2 Polymer Matrix 11
2.2.1 Polydimethylsiloxane (PDMS) 11
2.3 Piezoresistive Composites 13
CHAPTER 3 EXPERIMENT 20
3.1 Materials and Sample Preparation 21
3.1.1 Graphite-PDMS Composites 21
3.1.2 Nickel-PDMS Composites 22
3.2 Characterization and Instrumentation 23
3.2.1 Mechanical Test 23
3.2.2 Resistance Test 25
CHAPTER 4 Results and Discussion 27
4.1 Piezoresistivity Property Under Tensile Tests 27
4.1.1 Monotonic Quasi-static Tensile Test 27
4.1.2 Cyclic Uniaxial Tensile Test 29
4.2 Piezoresistivity Property Under Compressive Tests 33
4.2.1 Monotonic Quasi-static Compressive Test 33
4.2.2 Cyclic Uniaxial Compressive Test 38
CHAPTER 5 Conclusion and Future Work 42
5.1 Research Conclusions 42
5.2 Recommendation for Future Work 44
REFERENCES 47
APPENDICES 55

LIST OF TABLES

Table 3-1 Graphite-PDMS composites fabricated in experiment with controlled variables 22

Table 3-2 Nickel-PDMS fabricated in experiment with controlled variables 23

Table 5-1 Summarizes the piezoresistive response to tensile/compressive strain of each sample fabricated in experiment.....43

LIST OF FIGURES

Figure 2-1 Schematic diagram of graphite structure.....6

Figure 2-2 Schematic diagram of nickel structure.....9

Figure 2-3 Schematic diagram of PDMS chemical structure.....12

Figure 2-4 Illustration of piezoresistivity due to geometry change.....14

Figure 2-5 Piezoresistivity characterization of introduced MEMS force sensor.....19

Figure 3-1 Uniaxial tensile tests with DIY stretch machine.....24

Figure 3-2 (a) DIY uniaxial compressive test machine (b) Circuit diagram of current-limiting method (c) Current-limiting method used to measure piezoresistivity.....26

Figure 4-1 Tensile strain tests result comparison between Nickel-PDMS and commercial piezoresistive sheet.....28

Figure 4-2 83% Nickel-PDMS composite resistance change with tensile strain.....30

Figure 4-3 Purchased sheet resistance change with tensile strain.....31

Figure 4-4 A schematic model for the change of conductive structure in the composites under pressing: the conductive fillers disperse randomly in the composite.....32

Figure 4-5 (a) Uniaxial compressive strain test result (b) Uniaxial compressive test result with logarithmic response.....35

Figure 4-6 Uniaxial compressive strain tests result comparison between Nickel-PDMS and commercial sheet.....37

Figure 4-7 Constant strain cyclic compressive test: normalized electrical resistance changes of 83% Nickel-PDMS versus time in response to three cycle loading – unloading of 10% strain.....38

Figure 4-8 Constant strain cyclic compressive test: normalized electrical resistance changes of commercial sheet versus time in response to three cycle loading – unloading of 10% strain.....39

Figure 4-9 Piezoresistivity response of Nickel-PDMS under minor-pressure compressive strain cyclic test.....40

CHAPTER 1: INTRODUCTION

1.1 Introduction

Flexible and stretchable piezo-resistive composite have drawn great attention in extensive fields for its ability of transforming applied physical parameters into corresponding quantified electrical resistance change. Compared to traditional rigid electrical sensors, its outstanding merits of facile fabrication and deformability give this new material broad potential for applications in many emerging industries such as health monitoring, motion detection, entertainment [1,2] and robot control. The piezo-resistive composite is generally composed of two components: a conductive filler and a polymer matrix. Wide range of materials have been examined to add into the composite in order to combine their intrinsic features and widen the application area. Rubbery materials including polydimethylsiloxane (PDMS) [3], silicone rubber (SR) [4] and acrylonitrile butadiene rubber (NBR) [5] are commonly adopted as the supporting polymer matrix for their excellent flexibility and elasticity. Several prior articles have researched in this area by dispersing conductive fillers into the polymer matrix evenly to achieve the piezo-resistive effect. Wu et al. [6] have reported piezoresistive strain sensors with both strain and pressure sensing capabilities composed of graphite exhibiting high gauge factor and self-healing characteristics under large deformation. Zhao et al. [7] have researched the high piezo-resistive performance sensors based on graphite nanoplatelet−carbon nanotube hybrids/polydimethylsilicone (GCHs/PDMS) composites, whose demonstrated ultralow percolation threshold and high sensitivity met the demand of typical wearable sensors. Canavese et al. [8] presented flexible and easy conformable piezo-resistive material composed of Nickel and variable polymer bases with optimized micro-casting and hot embossing techniques and achieved up to nine orders of electrical resistance change when subjected to a mechanical

pressure, providing suitable tactile sensing ability on robot surface. It can be observed from those previous works that the mainstream of experimental conductive fillers of piezo-resistive material can be categorized into two types: metal [9-11] and non-metal [12] elements. Copper and Nickel are most commonly used metal elements in this area, and we can conclude from prior results that Nickel has shown better performance compared to copper in various tests [13,14]. Results indicates that Nickel composite is more sensitive than equivalent Cu composite. This phenomenon is believed to be the consequence of different oxidization rates between two metal elements [15]. While in non-metal element selections, carbon material includes graphite [16], graphene [17], carbon nanotube [18] and carbon black [19] have been researched most often as the conductive filler. Graphene and carbon nanotube were all demonstrated to be effective filler components in previous studies with abundant sensitivity. However, their practical application has been severely impeded by unsatisfying cost performance. Graphite, on the other hand, is a ubiquitous inexpensive material which provides sufficient improvement in electrical conductivity of the final composite. Nag et al. [20] presented a unique design and fabrication method for graphite/PDMS sensors for biomedical application. The new 3-D printing technique furthermore decreased the patterning cost while providing adequate sensing ability, increasing the chances of utilizing this composite in future biomedical world.

In this study, we present the fabricating and measuring processes for a flexible, low cost Nickel/Graphite-PDMS piezo-resistive composite with high sensitivity and favorable repeatability under uniaxial compressive and tensile force. The final composite performance was compared with current commercial piezo-resistive material in different aspects. Subsequently, we investigated into the possibility of applying the new composite into wearable motion-detecting sensors, demonstrating its promising potentials in commercial purpose.

1.2 Motivation and Objectives

As is discussed above, the extraordinary characteristics of piezoresistive deformable sensors have attracted wide attention from both industries [21,22] and academics [17]. In the past decade, many efforts have been devoted into this area and much progress have been achieved. However, accompanied by the advancement of experiments and understanding of this new material, limitations have also been discovered. For example, carbon-nanotube-based polymer nanocomposites piezoresistive strain sensors gave outstanding sensitivity and wide response range but with limited repeatability [23]. While CNT yarn sensors demonstrated excellent stability and repeatability in response to strain change, yet very low gauge factor was reported [24]. Although outstanding features including sensitivity, mechanical strength, stability, economic efficiency and repeatability have been reported in quite a few studies, there is little report on fabrication methods that can incorporate all those traits. Thus in the current application and production phase that each specific product lay particular stress on certain characteristic. Also, zero drifting is a commonly reported issue exists in many studies that describes an unstable electrical resistance reading of the composite at an initial free-loading stage. These prevailing problems, even though may not hold back the main piezoresistive performance of the products, still prevent the broad application of the flexible and stretchable piezoresistive composites. Consequently, our motivation of this study is to introduce a novel fabrication method for a flexible strain sensor made from piezoresistive composite material that can achieve the best balance between convenience, performance and economic efficiency.

In this context, this thesis describes efforts to: 1) Introduce a convenient fabrication method to evenly mix conductive filler and polymer matrix into flexible and stretchable piezo-resistive material. 2) Evaluate the electrical resistance response when applying external strain

and the corresponding piezo-resistive performance with various types of mechanical tests. 3). Compare and analyze the acquired experiment data from different sets of material and conclude with final design scheme that achieves the best overall performance.

CHAPTER 2: LITERATURE REVIEW

2.1 Conductive Filler

2.1.1 Graphite

Carbon is a ubiquitous polymorphic material. It exists in three different forms: graphite, diamond and fullerenes. Graphite mainly differs from diamond in that its carbon bonding consists of sp^2 (trigonal) hybridization instead of sp^3 (tetrahedral) hybridization. The different bonding structures determine their different atomic structure, where graphite consists of carbon layers (also known as graphene layers) and diamonds consists of a three-dimensional crystal structure. Based on its layer-shape structure constitution, graphite demonstrates significant anisotropic electrical/thermal conductivity: the electrical/thermal conductivity has been proven to be excellent with-in the layers due to the in-plane metallic bonding while only being a poor conductor at the perpendicular direction with respect to the carbon layer plane because of the weak Vander Waals force between the layers. As a result of this distinct electric/thermal characteristic in different direction, graphite has been widely used in electro-chemical electrodes and electric brushes. The outstanding anisotropy and high selectivity in the stress direction is another reason we adopt graphite as our strain sensor filler.

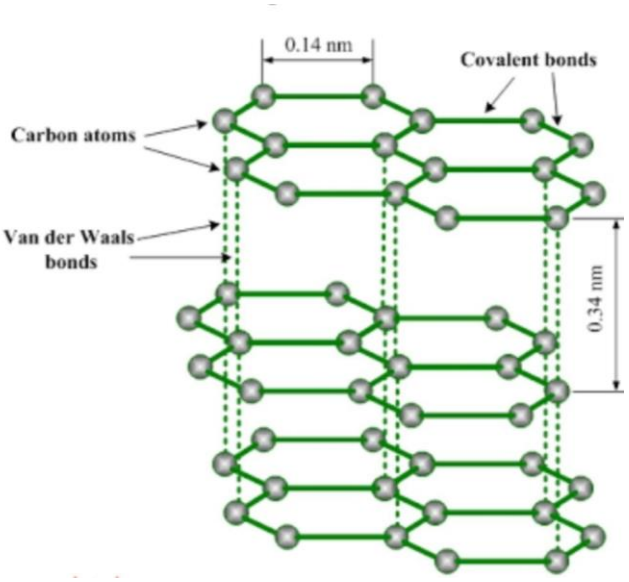

Figure 2-1 Schematic diagram of graphite structure.

Within the layer structure of graphite, the atoms are aligned in a hexagonal pattern while the layers are stacked in the AB sequence [25]. This leads to the hexagonal unit cell structure of graphite where we can calculate the dimension of the unit cell as c = 6.71 Å and a = 2.46 Å [26]. The structure of graphite consists of a succession of layers parallel to the basal plane of hexagonally linked carbon atoms as shown in Fig 2.1. In this stable hexagonal lattice, the in-plane bond (interatomic) length is 0.14 nm and the between-plane distance is 0.34 nm. Crystal density is 2.266 g/cm^3 as compared with 3.53 g/cm^3 for diamond. In the graphite sp^2 hybridization structure, regular covalent bonds that connect contiguous carbon atoms only exist in three out of four carbon valence electrons. The isolated electron (π electron) will resonate between the rest valence bond structures. Thus, the chemical bonding force within-plane can reach up to 150-170 kcal/[gram/atom] while the between-plane chemical bonding force is only 1.3-4 kcal/[gram/atom], which is about 2% of the former. The noteworthy difference between the bonding forces is usually attributed to the result of van der Waals forces and this distinct weak

between-layer force has led to several unique characteristics of graphite: 1) the tendency of graphitic materials to fracture along planes, 2) the formation of interstitial compounds and 3) the lubrication and compressive properties of graphite. These special characteristics of graphite determine its own application and limitation. In our study, the compressibility and anisotropy of graphite are valued while its fragility can be a great disadvantage. In light of this, research and modification in appropriately applying this material into our strain sensor application will be further explained.

In order to achieve a stable and unified graphite source, we decided to choose commercial graphite powder for our experimental use. Sources of commercial graphite include both natural graphite mined from rock and synthetic graphite manufactured from other carbonaceous materials. For commercial purposes, natural graphite is classified into the following three categories, according to its crystallinity, grain size, and morphology: amorphous, crystalline (flake), and crystalline (lump or chip). These commodity classes differ in the level of purity of the graphite, the proposed industrial use, the price, and the geologic setting in which the graphite occurs.

The graphite powder used in this study was purchased from US Research Nanomaterials, Inc., a high-tech enterprise focusing on research and development of nanotechnology which is considered a stable and reliable supplier of nanomaterial. We chose 25um natural graphite spherical powder, super fine, 99.95% in the experiment. It has the property of high-quality natural crystalline graphite, oxidation resistance at high temperature, self-lubrication and plasticity, as well as good electrical conductivity, electro heat property and adhesion.

Research and applications on novel graphite composite fabrication methods have recently drawn a lot of attention. Feng et al. [27] reported a new fabrication approach for a

graphite/polypropylene (PP) composite with high thermal conductivity due to the effective continuous thermally conductive network constructed with graphite flakes. In this work, the thermal conductivity coefficient of the graphite/PP composites was markedly improved to 5.4 W/mK at a graphite loading of 21.2 vol %, which is attributed to the occurrence of orientations of crystalline graphite flakes with large particles around PP resin particles and the formation of a perfect thermally conductive network. The author used the Hashin-Shtrikman (HS) model to explain the outstanding thermally conductive property of the graphite/PP composites. Sun et al. [28] developed a black phosphorus nanoparticle-graphite composite by mechanochemical reaction in a high energy mechanical milling process. This method produces phosphorus–carbon bonds which are stable during lithium insertion/extraction. Excellent electrical connection between phosphorus and carbon was demonstrated in this design. Motozuka et al. [29] investigated the fabrication of copper–graphite composites with a centrifugal ball mill. The copper particles were homogeneously milled in a graphite vessel with varied reaction time. The produced composites were later compared with pure graphite and pure copper particles. Test results suggests that the interfacial bonding between the copper and graphite was attributed to a Van der Waals attraction and/or binding force due to oxygen atoms located at the interface. Rohatgi et al. introduced a process for producing a copper alloy composite containing dispersed graphite. The process comprises locating compacted uncoated graphite in a preheated die, pouring molten copper alloy over the compacted graphite and infiltrating the compacted graphite with the molten copper alloy.

2.1.2 Nickel

Nickel is a silver-white lustrous metal with excellent hardness and tenacity. The Vickers hardness of Nickel is up to 638 MPa (material's ability to resist plastic deformation from a

standard source) and the Mohs hardness is measured to be 4.0 (qualitative ordinal scale characterizing scratch resistance of various minerals through the ability of harder material to scratch softer material). Large pieces of Nickel are found to have a rather low reacting rate with air under standard conditions due to the oxide layer on the external surface, while pure powdered Nickel demonstrates significant chemical activity by maximizing the reactive surface area. Even though Nickel is abundantly present on our planet, pure Nickel is rarely seen in nature; in most cases it is discovered in combination with sulfur and iron in pentlandite, with sulfur in millerite, with arsenic in the mineral nickeline, and with arsenic and sulfur in nickel galena[30]. The use of Nickel began long ago in human history, the first application is believed to be traced back as far as 3500 BCE. Bronze discovered in what is now Syria has been found to consist of at least 2 percent of Nickel [31]. The white copper mentioned in ancient Chinese manuscripts between 1700 and 1400 BCE is also believed to refer to Nickel alloy [32]. Another unique feature of Nickel is its magnetism: it is one of only four elements that are magnetic around room temperature. The Curie temperature of Nickel is 671 °F, which indicates that a large piece of Nickel will lose its magnetism above it.

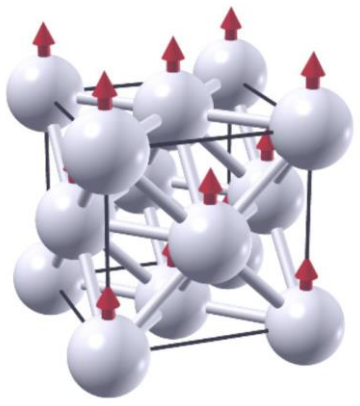

Figure 2-2 Schematic diagram of nickel structure.

The basic structure of Nickel is a face-centered cube with lattice parameter of 0.352 nm and an atomic radius of 0.124 nm. The three-dimensional schematic diagram of Nickel is shown in Figure 2.2. The face-centered crystal structure is stable enough to resist pressure up to 70 GPa. The ideal compressive strength of Nickel crystal is high up to 34 GPa. However, this limit can hardly be achieved by real bulk material due to the formation and movement of dislocations and is most seen in Nickel nanoparticles. The electrical and thermal conductivity of Nickel are also outstanding: 90.9 W/(m·K) and 69.3 nΩ·m respectively at room temperature. The unique physical characteristics of Nickel described above drive the growing attention it has received in modern industrial researches. Johnson et al. [13] presented a novel nickel nanostrand-silicone composite material at an optimized filler concentration demonstrates a dramatic piezoresistive effect with a negative gauge factor. A quantum tunneling percolation model was also established to accurately predict the mechanical and thermal trends of this material. Chen et al. [33] reported a new electrodeposited nickel/carbon nanotubes composite fabrication method. By co-depositing carbon nanotubes suspended in an electrolyte with growing nickel during electrodeposition, a saturation concentration for dispersing carbon nanotubes and relationship between carbon nanotube co-deposition and carbon nanotube concentration were discovered and examined. Kuang et al. [34] demonstrate that by electrodeposition in a nickel sulfamate solution with graphene oxide (GO) sheets in suspension, with appropriate graphene content, the thermal conductivity of the composite can exceed 15 percent of that in pure nickel electrodeposits. Significant improvement was also demonstrated in the hardness measured by nanoindentation. Tench et al. [35] developed a new electrodeposited nickel-copper multilayer composite. The tensile strength of electrodeposited layered composites of the nominal overall composition 90 percent Ni-10 percent Cu is shown to increase sharply to the 1300 MPa range as the thickness of

the Cu layers is decreased below 0.4 ώm. This tensile strength value is almost a factor of three greater than that measured for Ni itself, and more than a factor of two greater than the handbook value for Monel 400.

2.2 Polymer Matrix

2.2.1 Polydimethylsiloxane (PDMS)

Polydimethylsiloxane (PDMS) (chemical formula as CH_3 $[Si(CH_3)_2O]_nSi(CH_3)_3$, where n is the number of repeating monomer $[SiO(CH_3)_2]$ units [36]) also known as dimethylpolysiloxane or dimethicone, is the most commonly used material in polymer in siloxane ("silicone") elastomers. The chemical structure of polydimethylsiloxane is shown in Figure 2.3. This elastomeric polymer has ideal properties such as nontoxicity, incombustibility, biocompatibility, elasticity, transparency, and durability. Additionally, flexibility of the polymer backbone in PDMS exposes its methyl group at numerous interfaces, which are low interacting substitute, thereby creating minimum level of interaction at their surface. PDMS has found extensive usage in numerous existing or potential applications. It is a widely used stamp resin in the procedure of soft lithography, making it one of the most common materials used for flow delivery in microfluidics [37] and creation of lab-on-chip devices [38]. By controlling the degree of cross-linking PDMS can be made exceptionally soft and its dimensions can adapt to mechanical changes in its surrounding environment in a resilient way for use in flexible medical devices and tissue engineering [39]. The stretchability of PDMS-based devices makes it a crucial component of various promising electronics including wearable devices and real-time health monitors [40]. It has also gained more and more attention in smart window applications as the so-called suspended particle devices due to its excellent optical clearance. Application of

Polydimethylsiloxane also includes contact lenses [41], water-repellent coatings [42], cosmetics [43], lubricants [44], and many others.

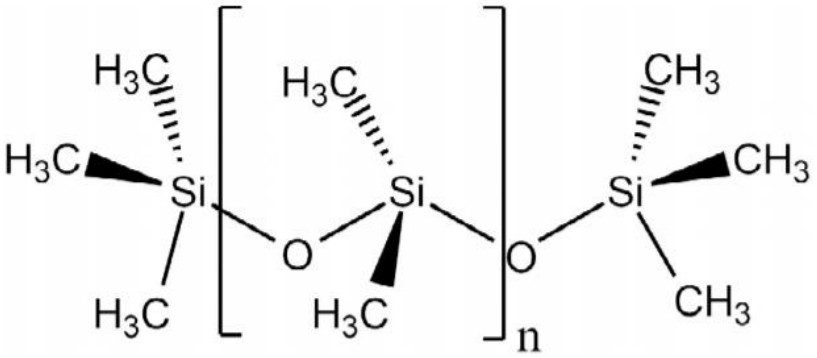

Figure 2-3 Schematic diagram of PDMS chemical structure.

Many studies have examined the performance of Polydimethylsiloxane on piezoresistive composite and the relevant applications. Niu et al. [45] reported a strain and pressure sensitive flexible piezoresistive sensors based on nanocomposites of graphene nanoplatelets (GNPs) and Polydimethylsiloxane (PDMS) elastomer. The strain detective sensors show positive piezoresistive characteristics under diverse levels of static strain up to 20% due to the flexibility and stretchability of PDMS elastomer. Since the GNPs/PDMS piezoresistive sensors can not only respond to subtle bending but also distinguish them accurately for detecting the finger motions, the GNPs/PDMS nanocomposite is a good candidate for artificial skin and wearable sensor applications. Stassi et al. [11] presented a novel fabrication method for a low cost and highly mechanically flexible 8x8 pressure matrix sensor with dedicated electronics using an innovative metal-Polydimethylsiloxane composite material. Under the action of a compressive stress the material exhibits a strong piezoresistive effect varying its electrical

resistance by several orders of magnitude. The sensor was tested with a customized electronic circuit after an exhaustive characterization of the functional properties of the material. Lu et al. demonstrated the characterization of piezoresistivity of Conductive Polydimethylsiloxane (CPDMS) and the corresponding fabricating process for a parylene-coated, CPDMS Micro Fingerprint Sensor (MFS) with mushroom-shaped electrodes. With a gauge factor of about 7.4 and the piezoresistive sensitivity about $3x10^{-6}$ Pa^{-1} in the tensile test setup. Due to its excellent physical and chemical properties, we decided to use Polydimethylsiloxane as our main polymer matrix material.

2.3 Piezoresistive Composites

The piezoresistive effect is a change in the electrical resistivity of a semiconductor or metal when mechanical strain is applied. This was first discovered by William Thomson (Lord Kelvin), who observed the resistance change in copper-iron alloy when external strain was applied [46]. After that, pure metal or metal alloy became the main material of choice for the piezoresistive circuits which was applied in strain gauge and thermo-resistors until 1954 when Smith, a researcher in the renowned Bell Laboratories at that time, discovered the large piezoresistive effect in silicon and germanium [47]. Since then, piezoresistive sensors became a commonly seeing circuit on the commercial market and prevail in both academic and industrial applications.

In conducting and semi-conducting materials, changes in inter-atomic spacing resulting from strain affect the bandgaps, making it easier (or harder depending on the material and strain) for electrons to be raised into the conduction band. This results in a change in resistivity of the material. Within a certain range of strain this relationship is linear, so that the piezoresistive coefficient ρ_σ is constant and can be expressed as:

$$\rho_\sigma = \frac{\frac{(\partial\rho)}{\rho}}{\epsilon} \tag{1}$$

where $\partial\rho$ is the change in resistivity, ρ the original resistivity and ϵ the strain.

The resistance change in piezoresistive composites is mostly attributed to the geometry change of the material resulting from the applied external stress. To calculate the exact change, we assume a prismatic bar of uniform rectangular cross-section. Then we can calculate the resistance of the conductor using the formula below which is derived from the Ohm's Law:

$$R = \frac{\rho L}{A} \tag{2}$$

where ρ is the original resistance, L the conductor length and A the cross-section area of the current flow [48]. The conceptual diagram of this process is shown in Figure 2.4.

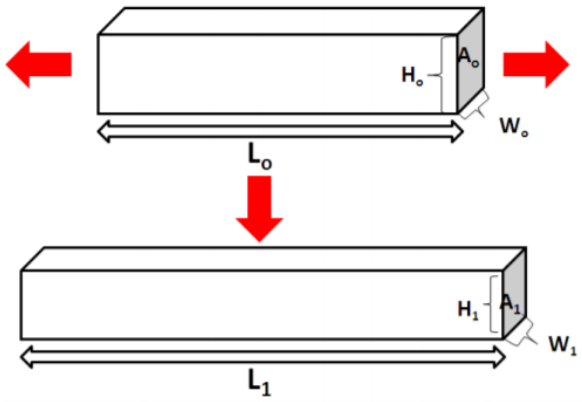

Figure 2-4 Illustration of piezoresistivity due to geometry change.

Differentiating (2) we obtain:

$$dR = \frac{\rho}{A}dL + \frac{L}{A}d\rho + \frac{\rho A}{L^2}dA \tag{3}$$

Dividing the (3) by resistance R yields,

$$\frac{dR}{R} = \frac{dL}{L} + \frac{d\rho}{\rho} + \frac{dA}{A} \tag{4}$$

The $\frac{dL}{L}$ term in the equation above indicates the fractional change of the length, $\frac{d\rho}{\rho}$ represents the fractional change in resistivity of the conductor resulting from applied force along the longitudinal direction and $\frac{dA}{A}$ part represents fractional change in area. Then we can get the relative change in length or the axial strain as:

$$\varepsilon_{axial} = \frac{\Delta L}{L} \tag{5}$$

and lateral strain as:

$$\varepsilon_{lateral} = \frac{\Delta W}{W} = \frac{\Delta H}{H} \tag{6}$$

Now we try to express the Poisson ratio with the terms above:

$$v = -\frac{\varepsilon_{lateral}}{\varepsilon_{axial}} \tag{7}$$

Then we can express the relative resistance change as a function of the strain and resistivity:

$$\frac{\Delta R}{R} = (1 + 2v)\varepsilon_{axial} + \frac{\Delta \rho}{\rho} \tag{8}$$

From the equation above we observe that the relative resistance change consists of two parts: $(1 + 2v)\varepsilon_{axial}$ as geometric component and $\frac{\Delta \rho}{\rho}$ as electronic component. In metal materials, the geometric component is usually the predominant source of piezoresistive behavior due to deformation, while in semiconducting materials, fractional change in resistivity, $\frac{\Delta \rho}{\rho}$, plays a more significant role in the overall resistance change.

The Gauge Factor (K) of a piezoresistive material is defined as the fractional change in resistance ($\frac{\Delta R}{R}$) per unit strain, ε. It is expressed as [48]:

$$K = \frac{\frac{\Delta R}{R}}{\varepsilon_{axial}} = (1 + 2v) + \frac{\frac{\Delta \rho}{\rho}}{\varepsilon_{axial}} \tag{9}$$

In metal materials, since the change induced by electronic resistivity is negligible, we can reduce the Gauge Factor to:

$$K_{metal} = \frac{\frac{\Delta R}{R}}{\varepsilon_{axial}} \cong 1 + 2v \tag{10}$$

For those metal materials, the Poisson's ratio generally ranges from 0.3 to 0.4, and Gauge Factor is around 2. When semiconductor materials are subjected to an external strain, symmetry of the crystal lattice is degenerated and as a result the carrier mobility and resistance change [49]. Electrical sensitivity in the atomic state and generation of high resistance difference determines that semiconductors are very suitable materials for piezoresistive sensors. Generally, semiconductors show relatively high Gauge Factors (around two orders of magnitude more than metals). Since the geometrical component ($v \cong 0.28$) of the Gauge Factor is not as high as the electronic component, it can be neglected and Gauge Factor can be written as:

$$K_{semiconductors} = \frac{\frac{\Delta R}{R_0}}{\varepsilon_{axial}} \cong \frac{\frac{\Delta \rho}{\rho}}{\varepsilon_{axial}} \tag{11}$$

Among various conducting composites, the underlying mechanism of piezoresistivity can be different. For some composites, instead of the geometry change due to the applied external mechanical pressure, the change in conducting network structure could have more significance in

the overall piezoresistivity behavior. The network structure change could result from a combination of change in inter-particle separation, and reorientation of filler particles [50].

$$Gauge\ Factor_{composites} = \frac{\frac{\Delta R}{R_0}}{\varepsilon_{axial}} \cong \frac{\frac{\Delta \rho}{\rho}}{\varepsilon_{axial}} \quad (12)$$

For composites, many external factors including mechanical, thermal or even environment can lead to change in the electrical resistance. In most cases, the main factor is the change of the internal composite structure such as the between-filler distance, number of the contact points and contact points density. With any of those above-mentioned factors applying to the composites, changes inside the structure including breakdown of the filler junctions or reformation of the conducting network by rotation/alignment/translation could take place [51]. If, as a response to external stimuli, the components of the composite filler separate from each other, the resistance will increase which is normally referred to as positive piezoresistance. On the other hand, if the between-filler distance was reduced by the stimuli, resistance will decrease producing as negative piezoresistance. The final dominant mechanism of the composite depends on various factors such as polymer type, filler type, concentration, geometry, filler orientation-dispersion, amplitude, direction and type of external factor, measurement configuration [52].

Piezoresistive composites have found application and commercialization in many areas from civil engineering to textiles as self-monitoring sensory materials because of their ability to reflect the magnitude of external factors in terms of change in resistance [53]. Piezoresistive composites are commonly used as the core material in different sensors including pressure sensors, strain sensors, tactile sensors and temperature sensors. Yan et al. [54] reported a highly stretchable graphene–nanocellulose composite nano-paper fabricated for strain-sensor applications. Three-dimensional macroporous nano-paper from crumpled graphene and

nanocellulose is embedded in elastomer matrix to achieve stretchability up to 100%. The stretchable graphene nano-paper is demonstrated for efficient human-motion detection applications. Luo et al. [55] presented a wearable sensor patch system that integrates flexible piezoresistive sensor (FPS) and epidermal electrocardiogram (ECG) sensors for cuffless BP measurement. This noninvasive and real-time cuffless blood pressure (BP) measurement realizes the idea of unobtrusive and continuous BP monitoring which is essential for diagnosis and prevention of cardiovascular diseases associated with hypertension. As compared to the current optical-based cuffless BP measurement devices, the sensing patch requires much lower power consumption (3 nW) and is capable of detecting subtle physiological signal variations, thus providing a promising solution for low-power, real-time, and home-based BP monitoring. Liu et al. [56] described the development of MEMS force sensors constructed using paper-based piezoresistive conductive material. The device is inexpensive, simple to fabricate, lightweight, and disposable. The final force sensor can achieve a measurement range of 15 g and a resolution of 0.39 g. The input/output piezoresistivity characterization with respect to folded/unfolded beam of the sensor is shown in Figure 2.5.

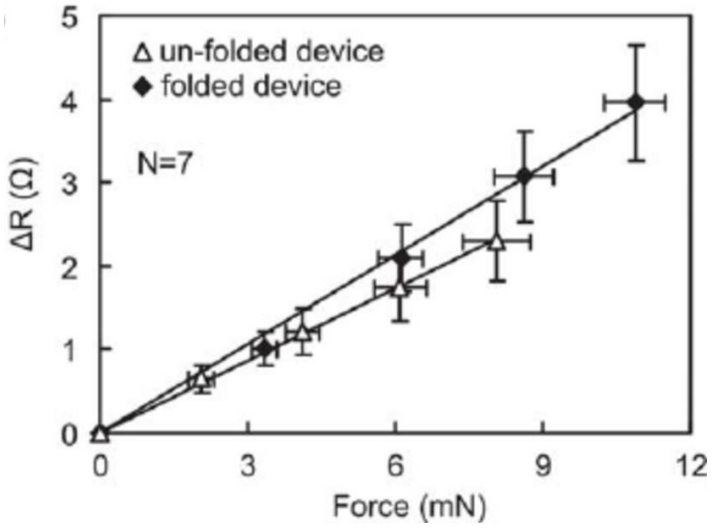

Figure 2-5 Piezoresistivity characterization of introduced MEMS force sensor.

CHAPTER 3: EXPERIMENT

The objective of this study is to develop a cost-efficient and high-performance uniaxial strain sensor based on Graphite/Nickel PDMS piezoresistive composites. In order to achieve our primary goal, the raw material in our experiment should meet the requirements of ubiquity and the fabricating technique required in processing should be inexpensive and easy-to-use. We dedicated efforts to improve the traditional processing method to be both time-effective and cost-effective by saving laboring and materials, thus optimizing the overall manufacturing output. According to relevant literature, a non-negligible issue that would severely interfere with the product quality is the uneven dispersion of the conductive filler. In order to tackle this problem, we added both mechanical stir and ultrasonic agitation (especially important in Nickel-PDMS composite since the metal powder aggregates due to its magnetism) into the mixing procedure. Air bubbles formed during the mixing procedure in composite samples are also commonly mentioned in many studies. Those bubbles will later cause small empty spherical cavities in composite samples and obstruct the piezoresistive performance by breaking up the conductive pathways. In our study, this is solved by placing the well mixed sample in vacuum pump until all the bubbles have been extracted, which usually takes around one hour depending on the material type and concentration. In addition, surface quality of the composite is crucial in the final performance since it determines the fit level between the sensor and the tested object. With respect to that issue, we spincoated the composite samples before the heat treatment to achieve the best surface quality with appropriate thickness. The overall experimental procedure can be broken down into four subsections: mixing, pretreatment, heat treatment and assembly. By comparing different methods and procedures, we have greatly simplified the manufacturing

process and reduced the difficulty in operation, paving the way for potential commercial applications and mass production.

3.1 Materials and Sample Preparation

3.1.1 Graphite-PDMS Composites

Graphite powder used in experiment was directly purchased from US Research Nanomaterials, Inc as Natural Graphite Spherical Powder, Super Fine, 99.95%. Two different sizes of graphite powder, 25 μm and 300μm respectively, were selected in order to examine the influence of powder radius on composite performance. The result of this comparison will be discussed along with other factors in the result section later. According to the recent research, the wet mixing method, which means the mixture obtained when water is added to filler in advance, will improve the dispersion of conductive fillers in PDMS. Thus we mixed the graphite powder with PDMS base at first place, and dispersed the filler evenly with mechanical stir at the speed of 75 rpm. Multiple graphite concentrations were selected to observe the effect on piezoresistivity, aiming to ease the experiment we used weight ratio to represent the concentration. Weight ratios of graphite powder ranging from 35% to 83.3% were tested separately. Then the PDMS cure (the weight ration of PDMS base: PDMS cure was 10:1) was added to the solution and ultrasonically agitated for 10 minutes. The vibrated solution was further mechanical stirred until homogeneous to ensure the graphite powder was evenly dispersed in PDMS. The solution was later transferred onto clean glass slides and degassed in a vacuum pump until all bubbles were extracted. Subsequently, the glass slides were heated at 200 ◦C for 20 hours then cooled to room temperature. The resulting graphite-PDMS composite sample was then cut into square shape sheets with side length of 8 mm and mounted on copper band by conducting resin for further tests. Details of fabricated graphite-PDMS are shown in table 3-1. It’s worth mentioning that

with limited knowledge of the effect of each fabrication parameter on experiment results that we acquired at the beginning of experiment, this details table does not reflect a comprehensive design of experiment but a exploratory experiment that aims to collect preliminary data for further optimization. This also applies to details table of other composite fabricated in this research.

Table 3-1 Graphite-PDMS composites fabricated in experiment with controlled variables

Graphite-PDMS Sample	Graphite Powder Size(μm)	Graphite Concentration(%)	Spincoat Settings(RPM*s)	Sample Thickness(inch)
GS1	3	35	1200 × 60	0.006
GS2	3	40	1200 × 45	0.004
GS3	25	40	1200 × 45	0.009
GS4	25	40	1200 × 60	0.006
GS5	25	40	800 × 45	0.009
GS6	25	40	800 × 60	0.008

3.1.2 Nickel-PDMS Composites

The nickel powder used in the experiment was also purchased from US Research Nanomaterials, Inc as Nickel Ni Powder. 99.5% with 10 μm diameter. Similar to graphite-PDMS composite, the nickel powder was first mixed with PDMS base but instead of mechanical stir we used ultrasonic agitation for 10 minutes. Due to the unique magnetism of Nickel powder, mechanical stir will cause powder to aggregate around the rotor instead of dispersing in solution

with negative effect in our experiment. Then the solution was mixed with PDMS cure and further ultrasonic agitated for 10 minutes to form a homogeneous solution. At this step, we want to mention that, in literature we saw some efforts to improve the nickel dispersion in PDMS by adding acetone as a wetting agent. However, in our experiment the result shows poor enhancement in the final piezoresisitivity so we omitted this process to simplify the manufacturing procedure. The solution was degassed for one hour later and heated at 100 ◦C for 20 h then cooled down to room temperature. The weight ratios of nickel we adopted in experiment range from 50% to 85.7% according to past studies. The composites were also cut into 8 mm × 8 mm sheet and mounted on copper band for further tests.

Table 3-2 Nickel-PDMS fabricated in experiment with controlled variables

Nickel-PDMS Sample	Nickel Concentration(%)	Spincoat Settings(RPM×s)	Sample Thickness(inch)
NS1	50	600 × 45	0.006
NS2	83.3	600 × 30	0.025
NS3	83.3	600 × 45	0.017
NS4	83.3	600 × 60	0.012

3.2 Characterization and Instrumentation

3.2.1 Mechanical Test

The stretch properties of samples in our study were tested with a customized equipment produced in the Automation Laboratory of North Carolina State University by measuring the real-time resistance of samples giving a specified extension and fixed time interval. The stretch

machine consists of a purchased lead screw and customized aluminum frame, as shown in Figure 3.1. A rotary knob was used to control the movement of the lead screw and four bolts were designed to fasten the specimens onto the machine. Samples were cut into a dimension of 40mm × 10mm and mounted with copper bands on both sides which were curved into a loop with the conductive side facing samples in order to eliminate the influence of different surfaces. The longer sides of the sample were oriented in parallel direction with the lead screw and have both ends of sample aligned with the edges of the fixture jaw. Stretch test starts with original length of 40 mm and no visible wrinkles or folds were observed on the surface. Samples were stretched 0.625% of their original length (0.25 mm) each time and after holding the stretch for 3 minutes the electrical resistance data was recorded three times at 30 seconds intervals. The electrical resistance of sample at each step is calculated as the average value of the three observations and upper/lower deviation were used to represent the stability of data. After reaching the peak length where fracture was about to happen, we shortened the samples to its original length using same methods and recorded the electrical resistance data. Then the samples were removed from the stretch machine and let stand for 30 minutes to relax the sample and the test was repeated two more times to observe the influence of cyclic stretch.

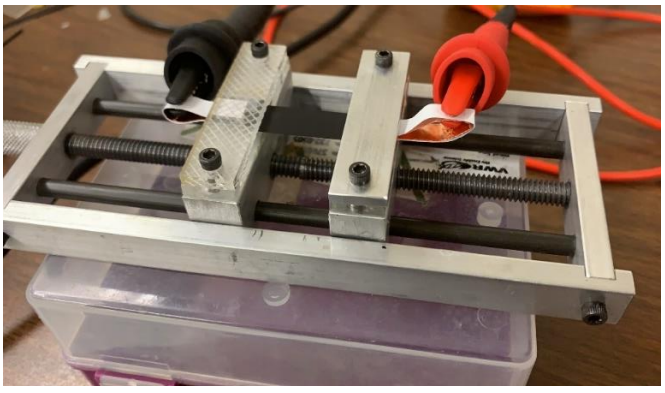

Figure 3-1 Uniaxial tensile tests with DIY stretch machine.

3.2.2 Resistance Test

As a key parameter in piezoresistivity assessment, electrical resistance of the sample under external pressure was tested with multiple methods including impedance meter, multimeter and data acquisition card. The produced graphite/nickel-PDMS composite along with purchased commercial piezoresisitive sheet were first cut into pieces with a dimension of 8mm × 8mm square sheet and then connected to copper band with a width of 6 mm by conductive gel in order to reduce the electrical resistance at the connecting points. Specimens were carefully placed at the center of the copper band to avoid the possibility of contact between copper bands on two surfaces when external force was applied and the corresponding interference of test result. Copper wires were then connected to the edge of the copper bands with conductive gel to avoid deformation or twist of sample when clamped by the multimeter clip. In compression test, the prepared samples were placed in a DIY compression test machine shown in Figure 3.2(a) below. The main body of the compression machine is a lead screw bought from market (AJS100-0.5K from Newport Inc.) with pitch of 0.254 mm (100 TPI). Then the lead screw was fixed to an aluminum outer frame with clearance of 0.5 inch in sample space. A protractor was mounted on the top surface of the compression machine fixed by glue to measure the rotation angle of the lead screw knob. The rotation angle was recorded and later converted into the axial feed distance of spindle or deformation of the sample. The prepared sample was placed at the center point of the bottom surface which is concentric to the lead screw at the beginning of each experiment. The sample did not contact with lead screw directly since stress concentration is inevitable when the sample has a larger dimension than the lead screw tip, hence a thin plastic sheet with a dimension of 10mm × 10mm was placed between the tip and sample to ensure an even spread of stress. Additionally, at the beginning of each test, the tip was lowered onto the sample surface

until the contact was firm and secured. Then when the readings of resistance on multimeter or impedance meter were stable, we began applying pressure onto the sample incrementally. This is essential because during the process of adding pressure onto sample, the resistance can fluctuate significantly due to the loose contact between tip and sample and this will take a toll on our experimental data. When using currently-limiting method, a constant voltage power supply(DC Regulated Power Supply 72-6628 from Tenma Inc.) that outputs 5V voltage was used as the main power source and a fixed resistance of 5.1 kΩ was set in the circuit along with the sample, the voltage of the sample was recorded and later converted to the resistance value. Then we used the multimeter to measure the resistance of the sample directly when compression force is applied, results showed little difference between those two methods so we decided to adopt the multimeter as the measurement directly. Impedance meter was also used in the experiment, but the interference of inductance and reactance suggests it is not the best choice.

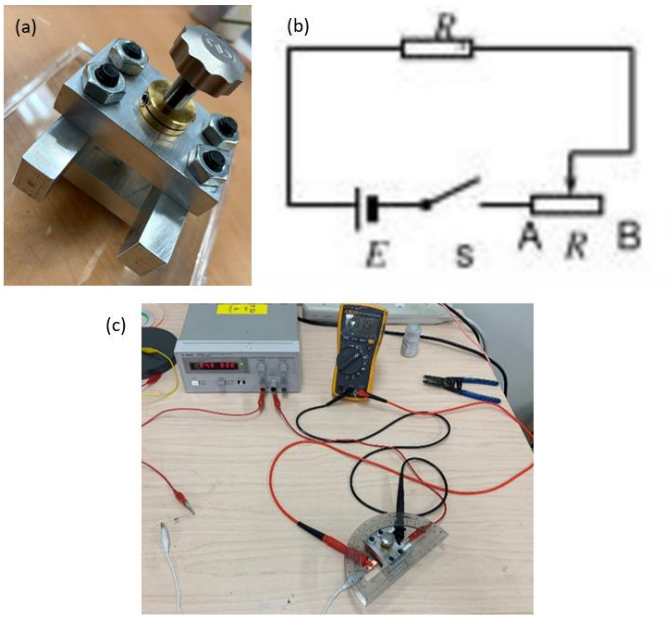

Figure 3-2 (a) DIY uniaxial compressive test machine (b) Circuit diagram of current-limiting method (c) Current-limiting method used to measure piezoresistivity.

CHAPTER 4: Results and Discussion

4.1 Piezoresistivity Property Under Tensile Tests

4.1.1 Monotonic Quasi-static Tensile Test

To understand the piezoresistivity of the composites, we first conducted tensile tests on both produced composite and purchased commercial pieoresistive sheet to explore the potential influence of mechanical deformation on the piezoresistivity performance. With samples cut to dimensions of 40mm × 10mm and fixed on the DIY stretch machine, electrical resistance data was measured when tensile strain was applied at a constant interval of 0.625%. However, due to the uneven tensile properties of samples, the yield strength and fracture strength differ. Hence the effective stretch range of each sample differ widely. For example, all the Graphite-PDMS sample we made have minimal elasticity, so fracture took place at very early stage of tensile tests and little meaningful data was collected. While for Nickel-PDMS composites, 83% weight ratio sample, regardless of their thickness, showed a rather obvious linear trend of resistance change when tensile strain was first applied. And the data adopted was sample NS2, 83% Nickel-PDMS composite with 0.025-inch thickness that was spin coated at 600 RPM for 30 seconds. When it comes to purchased commercial piezoresistive sheet, the elasticity was satisfactory, fracture took place at around 12% which is higher than that of our Nickel-PDMS composite that fracture at round 9% strain, yet the electrical resistance response to the strain change was less obvious than that of the produced samples. In the Figure 4.1 below, we recorded the mechanical tensile strain data($\Delta L/L_0$, ΔL – stretched sample length minus original sample length, L_0 – original sample length) vs. normalized resistance change ($\Delta R/R_0$, ΔR – the averaged real-time resistance minus original resistance, R_0 – original resistance before straining) along with the fitted linear trend of each data group.

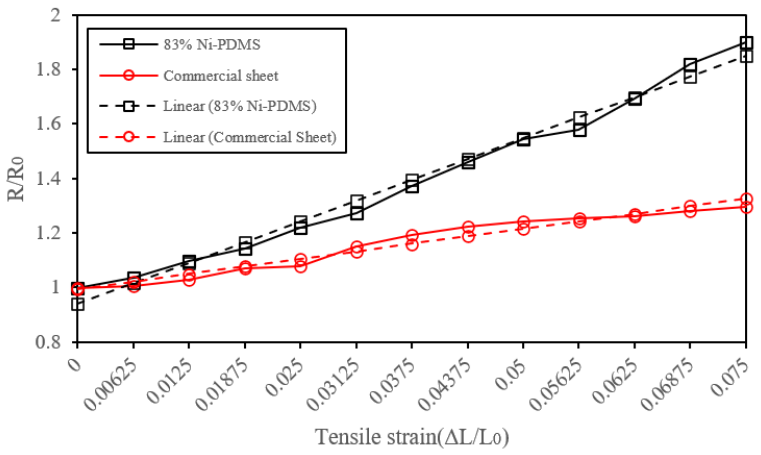

Figure 4-1 Tensile strain tests result comparison between Nickel-PDMS and commercial piezoresistive sheet.

It can be observed from Figure 4.1 that the resistance response for both tested samples were rather linear at the first trial. The fitted line for 83% Nickel-PDMS composite has a response functional equation as

$$y_N = 0.9393427 + 12.158934x \tag{13}$$

where y_N is the normalized electrical resistance $\Delta R/R_0$ of 83% Nickel-PDMS composite, x is the tensile strain $\Delta L/L_0$.

For purchased commercial piezoresistive sheet, the fitted functional equation is

$$y_C = 0.9942359 + 4.43149x \tag{14}$$

where y_C is the normalized electrical resistance $\Delta R/R_0$ of purchased commercial piezoresistive sheet.

Both fits presented above have R-square value that exceed 0.95 which means the fitted models accounted for more than 95% of the variation of the actual data and confirmed their credibility. With an almost tripled coefficient, our produced 83% Nickel-PDMS composite is

theoretically more responsive to tensile strain change on electrical resistance compared to commercial piezoresisitive sheet. On one hand, this phenomenon implies that potential tensile strain may have influence on the piezoresistivity performance of the produced composites. While on the other hand, it also suggested the possible application of this composite to tensile strain sensors. However, that idea need to be further examined with fatigue tests since as we mentioned before, the plastic strain is non-negligible on both materials which will often leads to irreversible shape deformation of the sample and inevitable disturbance to the piezoresistivity response.

4.1.2 Cyclic Uniaxial Tensile Test

In order to investigate the mechanical property of our piezoresistive composite and the potential application of tensile strain sensors, the electrical resistance change of the sample was measured repetitively and compared to that of the market-available commercial piezoresistive sheet (Pressure-Sensitive Conductive Sheet (Velostat/Linqstat) from Adafruit Industries). All the samples were cut into 40mm × 10mm pieces and placed on DIY stretch machine for cyclic tensile test. In preliminary tests, we found the tensile properties for either produced piezoresistive sample or purchased piezoresistive sheet were not ideal: they both reach to the yield strength and fracture strength with rather low external load. None of those samples can withstand up to 12% strain and plastic strain is estimated to take place above 5% strain. For our sample which was the 83% of Nickel-PDMS piezoresistive composite, this phenomenon was attributed to the high concentration of metal powder and low percentages of PDMS component. In sample preparation, a distinct tendency is that with the growing concentration of conductive filler, metal powder or carbon material, the produced samples show less elasticity and more likelihood of fracture. Thus at a high concentration of 83% weight ratio of nickel powder, the unsatisfactory tensile properties can be understood.

As mentioned above, low yield strength and fracture strength of samples determined that in repetitive tensile test, plastic strain of tested objective is inevitable and the initial absolute value drift of single sample's electrical resistance is foreseeable. To minimize the impact of this phenomenon on experiment result interpretation, we used relative electrical resistance change ($\Delta R/R_0$) in result analysis. Six repetitions of tensile test on our 83% Nickel-PDMS piezoresistive composite and purchased piezoresistive sheet along with the typical mechanical tensile strain ($\Delta L/L_0$, ΔL – stretched sample length minus original sample length, L_0 – original sample length) vs. normalized resistance change ($\Delta R/R_0$, ΔR – the averaged real-time resistance minus original resistance, R_0 – original resistance before straining) as a function of tensile strain are plotted below in Figure 4.2.

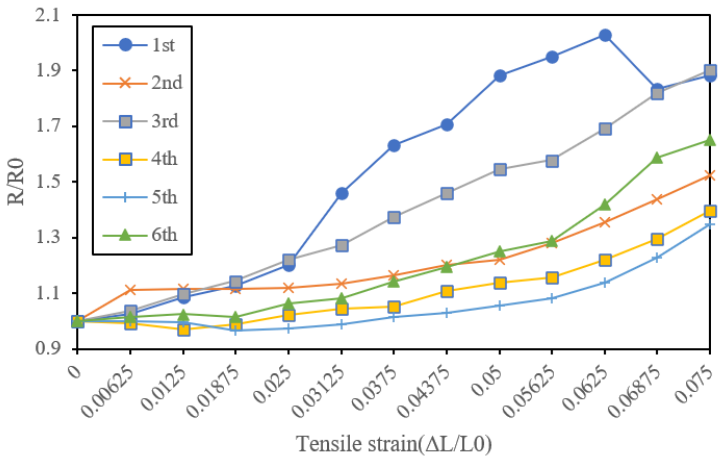

Figure 4-2 83% Nickel-PDMS composite resistance change with tensile strain.

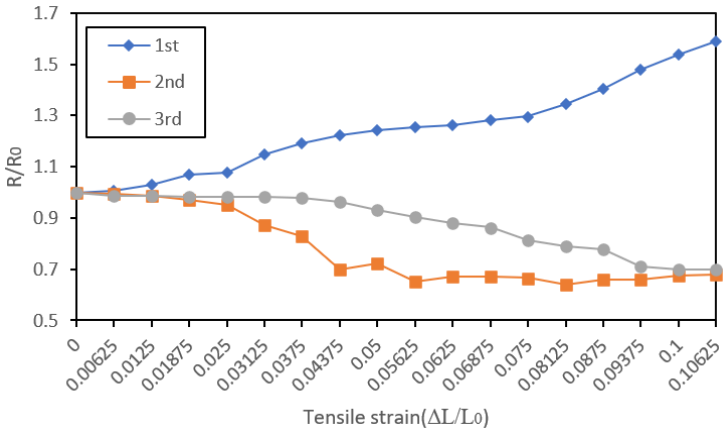

Figure 4-3 Purchased sheet resistance change with tensile strain.

In Figure 4.2, an obvious trend is that within the first 2.5% strain change, the electrical resistance of 83% Nickel-PDMS composite remain rather stable: the average normalized resistance of the six repetition only rise from 1 to 1.099 which is less than 1%. While the strain change ranges from 2.5% to 7.5%, the averaged resistance surged from 1.099 to 1.61 which is about 46.5%. This is considered to be the result of plastic strain of sample where in the latter several tests, the rectangle sample has been through essential deformation along the tensile direction and even after one hour rest of tests interval, the initial size of sample in each test beginning differs and the composite can no longer be effectively stretched along the length direction and compressed along the width direction to decrease the cross-sectional area and increase the length. Or as Chen et al. [57] suggested in their work, for the inner conductive particles to rearrange and form new conducting networks. However, it can be seen from the plot that, even for the latter 5% of strain change, the normalized resistance difference between each test is still non-negligible and no obvious variation trend with test sequence can be found. The only recognizable pattern in the plot is that, before the fracture took place, the overall electrical resistance grows as the tensile strain increase.

In tensile tests the commercial piezoresistive sheet cyclic tensile tests showed, higher fracture strain compared to the produced composite and a more disorderly pattern of strain-resistance response were observed. When testing commercial piezoresistive sheet, up to 10% strain change can be repetitively done without fracture taking place. For the first 2.5% strain change, a similar pattern to that of the produced composite was found, for this range of strain change, the averaged resistance of three test rise from 1 to 1.004 which is negligible, this is also attributed to the plastic strain of the sample due to the repetitive tests. However, for the rest of the tests, large resistance change was recorded without a uniform pattern: for the first test, the commercial sheet showed similar response to the produced sample while for the latter two tests, the pattern was completely different. This is considered to be due to the fact that when searching for appropriate commercial piezoresistive sheet, uniaxial compressive strain sensor was set as the primary goal. Thus as was described on the website, this piezoresistive sheet was specially designed for uniaxial compressive sensitive.

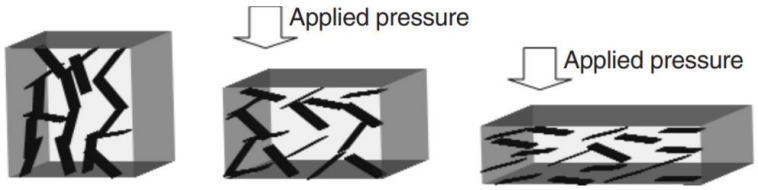

Figure 4-4 A schematic model for the change of conductive structure in the composites under pressing: the conductive fillers disperse randomly in the composite.

Generally speaking, the tensile properties of both produced composite and purchased piezoresistive sheet were not satisfactory. This test warned us that in uniaxial compressive

experiments and applications, we should avoid stretching the sheet in the longitudinal direction to minimize the impact of this property on piezoresistivity performance.

4.2 Piezoresistivity Property Under Compressive Tests

4.2.1 Monotonic Quasi-static Compressive Test

Since the primary application of our piezoresistive material design is compressive strain sensor, a large proportion of our effort was devoted into compressive strain tests. All the composite materials produced in the experiment were prepared and tested with multiple methods to evaluate their electrical resistance responses to changing external compressive stress and strain. However, not all of them demonstrated the desired response result due to different underlying issues. According to previous studies, piezoresistivity response of different materials can be attributed to three primary categories: a) the intrinsic piezoresistivity of material due to its physical/chemical structure change in respond to external strain, b) variation of contacting inter-particles electrical resistance, c) tunneling resistance change between neighboring particles due to inter-distance change caused by cracking or relative motions. Hence, even though different materials show similar piezoresistivity performance or non-piezoresistivity performance, it is still necessary to discuss them separately. For example, as our experiment shows, piezoresistivity of carbon composites decreases with increased carbon material concentration while that of nickel composites increase with nickel concentration. We consider the decreased piezoresistivity in carbon composites to be the result of increased viscosity of mixed solution when we were about to stir them evenly. Due to the limited mixing approaches including ultrasonic oscillation, magnetic rotor stirring and manually stirring, when concentration of carbon materials exceeds a threshold (as experiment indicates the threshold is weight ratio around 45%) the mixture of Graphite-PDMS cannot be effectively mixed evenly and the clusters lead to countless tiny gaps

between conductive pathways, and hence to poor piezoresistivity of the composites. While in Nickel-PDMS materials, the piezoresistivity increases with the growth of metal powder concentration because with much higher density compared to graphite, the nickel powder takes up only a small proportion of volume in the composites, thus low percentages of nickel will leave long distance between each nickel particle and require extremely high strain to reveal its piezoresistivity. Hence in our result analysis, only selected sample test results that provided proper performance will be discussed.

Graphite-PDMS composites were first studied using the data from 35% and 40% Graphite-PDMS composite which were both spincoated with 1200 RPM for 60 seconds and thickness of 0.006 inch. The data was obtained by placing the samples which were cut into 8mm square pieces onto the DIY compression test machine and applying compressive strain by driving the lead screw with certain angle intervals. The test results that consists of normalized electrical resistance ($\Delta R/R_0$, ΔR – the averaged real-time resistance minus original resistance, R_0 – original resistance before straining) response to strain change ($\Delta H/H_0$, ΔH – original sample height minus compressed sample height, L_0 – original sample height) are shown in Figure 4.5(a).

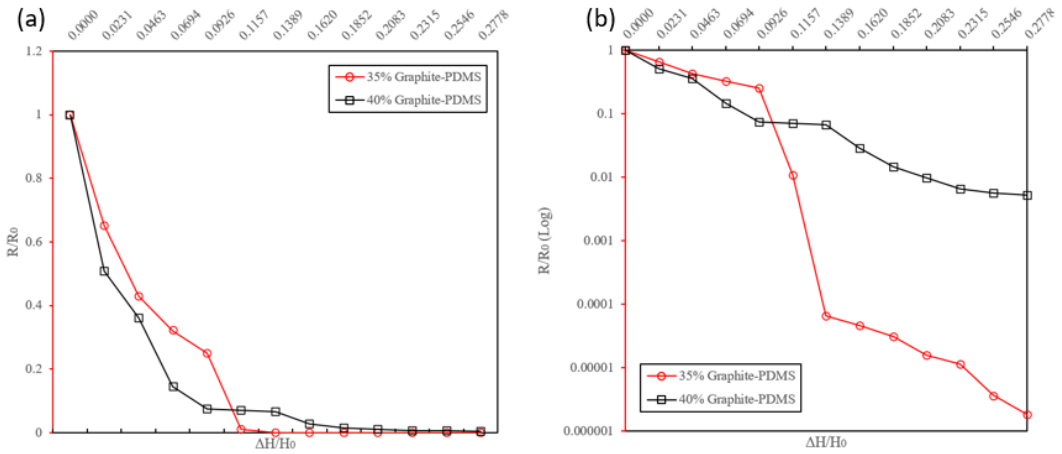

Figure 4-5 (a) Uniaxial compressive strain test result (b) Uniaxial compressive test result with logarithmic response

.

The strain change represented in x-axis ranges from 0% to 28% since beyond 28% the electrical resistance of both samples remains relatively stable level regardless of strain change. It can be observed from the plot that both samples showed similar trend when compressive strain increase. For the first 10% strain change, they both experienced rapid resistances drop while 40% Graphite-PDMS composite drops more rapidly than 35% (40% Graphite-PDMS composite resistance drops 23.5% faster than that of 35% in the first 10% strain change). After this period of decrease, the resistance remains at a low level compared to the original electrical resistance. Considering the initial resistances of both 35% and 40% Graphite-PDMS composites reach up to 10^6 Ω which increased the difficulty for us to interpret the resistance change after the plummeting stage, we added a logarithmic plot using the same data as Figure 4.5(b). From this log plot we can observe that even after the first 10% strain change, the resistances of both materials are still decreasing. For 40% Graphite-PDMS composite, the electrical resistance dropped about 2 orders of magnitude within the 28% strain change while for 35% composite, the drop was up to 6 orders which is rather impressive. As is mentioned before, this phenomenon

was attributed to proper conductive filler concentration in mixture that evenly spread the graphite powder into the composite, allowing the formed viscoelastic conductive matrix to better respond to external compressive strain compared with other composites.

Another point needs to be mentioned is that, for the first 10% strain change, both materials showed excellent linear response in electrical resistance. For 35% Graphite-PDMS, the fitted linear function is

$$y_{35\%} = 0.0206016 - 12.144272x \quad (15)$$

where $y_{35\%}$ is the normalized electrical resistance $\Delta R/R_0$ of 35% Graphite-PDMS composite, x is the compressive strain $\Delta H/H_0$.

For 40% Graphite-PDMS, the fitted linear function is

$$y_{40\%} = -0.027579 - 6.5349852x \quad (16)$$

where $y_{40\%}$ is the normalized electrical resistance $\Delta R/R_0$ of 40% Graphite-PDMS composite.

The R-square value for both fit reaches up to 98.5%, demonstrating the strong linearity in piezoresistivity response of the Graphite-PDMS composites. This important finding suggests a promising potential of this kind of material for use as a moderate compressive strain sensor with both high sensitivity and accuracy.

The electrical resistance response of Nickel-PDMS composite and purchased commercial piezoresistive sheet was studied together since they share similar piezoresistivity response pattern. Nickel-PDMS samples selected including 83% Nickel-PDMS composites NS2, NS3 and NS4. Samples were cut into 8mm × 8mm square pieces and fixed on DIY compression machine, response data was recorded by multimeter connected to the copper band on edges of samples and shown below in Figure 4.6.

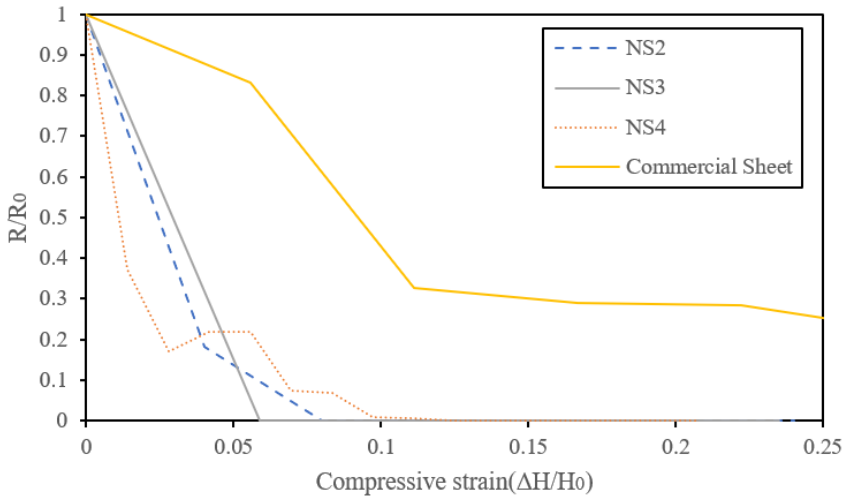

Figure 4-6 Uniaxial compressive strain tests result comparison between Nickel-PDMS and commercial sheet.

Figure 4.6 indicates that Nickel-PDMS composite with different thickness had similar piezoresistivity response patterns. Sheer decrease of electrical resistance was observed in every sample at the first 10% compressive strain change. However, for those three samples, NS4 shows best sensitivity to compressive strain compared to others. The electrical resistance of NS4 dropped to almost 10% of its initial resistance under only 3% of strain change. Compared with commercial piezoresistive sheet, whose electrical resistance dropped only 75% with up to 25% strain change, our produced 83% Nickel-PDMS composite obviously has better piezoresistive sensitivity. However, the commercial sheet sees its resistance drop in a larger range; from the plot we can observe that the response was steady declining after 10% strain change where the Nickel-PDMS has reached a stable zone and barely responds to the external stress anymore. Hence in general, our Nickel-PDMS composite shows excellent sensitivity to strain change over a limited response range.

4.2.2 Cyclic Uniaxial Compressive Test

Having examined the piezoresistive characterization of the produced composites, we still need to conduct cyclic uniaxial compressive tests to check whether repetitive usage of the composites will take a toll on or even cause permanent damage to its piezoresistivity performance. 83% Nickel-PDMS sample and commercial piezoresistive sheet were prepared and tested in the same manner discussed in previous section. The cyclic uniaxial compressive test was conducted by repeating the monotonic quasi-static compressive test for three cycles with unloading process. A single test cycle was repeated every 240 seconds with 10% compressive strain applied to the sample in each cycle. Figure 4.7 and Figure 4.8 shows the piezoresistive responses of the Nickel-PDMS composite and commercial sheet under cyclic loading and unloading processes.

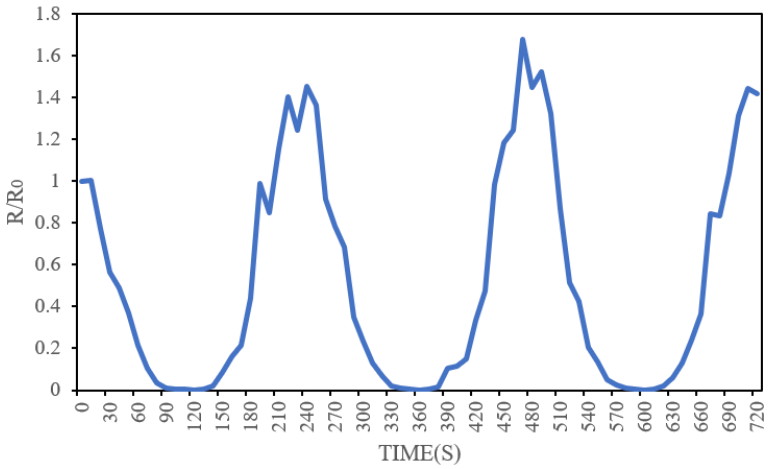

Figure 4-7 Constant strain cyclic compressive test: normalized electrical resistance changes of 83% Nickel-PDMS versus time in response to three cycle loading – unloading of 10% strain.

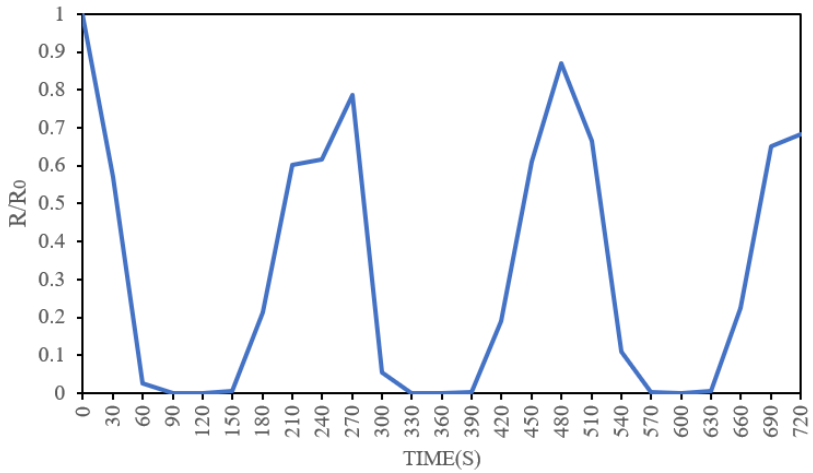

Figure 4-8 Constant strain cyclic compressive test: normalized electrical resistance changes of commercial sheet versus time in response to three cycle loading – unloading of 10% strain.

The normalized resistance changes in Figure 4.7 and Figure 4.8 indicate stable piezoresistivity performance for both samples. No abrupt resistance drift was detected in experiment within several circles which suggests that our piezoresistive samples obtained satisfactory repeatability when working under proper range of strains. However, the plots also shows that in repetitive usage, the initial resistance which was measured in the static situation may not always maintain the peak resistance value: in Graphite-PDMS experiment, the peak value in repetition is 43.9% higher than static initial resistance while in commercial sheet test, the peak resistance value is 27.7% lower than static initial resistance. This phenomenon is attributed to the difference between static measurement before tests and dynamic measurement in experiment. However, this issue would not affect its application of compressive strain sensor since during cyclic tests, the peak resistance and variation tendency in work are rather stable. Yet further adjustment and analyzing of this situation is still needed to minimize the potential noise.

The cyclic compressive strain response demonstrated in this experiment proved the Nickel-PDMS piezoresistive composite produced in our experiment can meet the needs of many

promising application. For example, modern industrial robot arms need to decide the proper grip power when clamping or grasping objects, this kind of mild to moderate compressive strain detection tasks meet the advantages and disadvantages of this material right to the point.

Considering the swift change of resistance at very early stage of applied strain, we also conducted tests of the piezoresistivity responses of Nickel-PDMS composites on minor external pressure to check if more accurate and sensitive compressive strain sensor is applicable. This minor stress tests is conducted based on 83% Nickel-PDMS composites that was cut into rectangle sheet with a dimension of 90mm × 77mm. Composite sheet was sandwiched between two aluminum sheets whose sizes slightly exceed that of the composite to ensure the weight was spread evenly on the composite. Five 45-gram weights were then placed on the center of the rectangle sheet one after another with interval of 30 seconds. Five cycles of tests were completed and the response data was collected as shown in Figure 4.9 below.

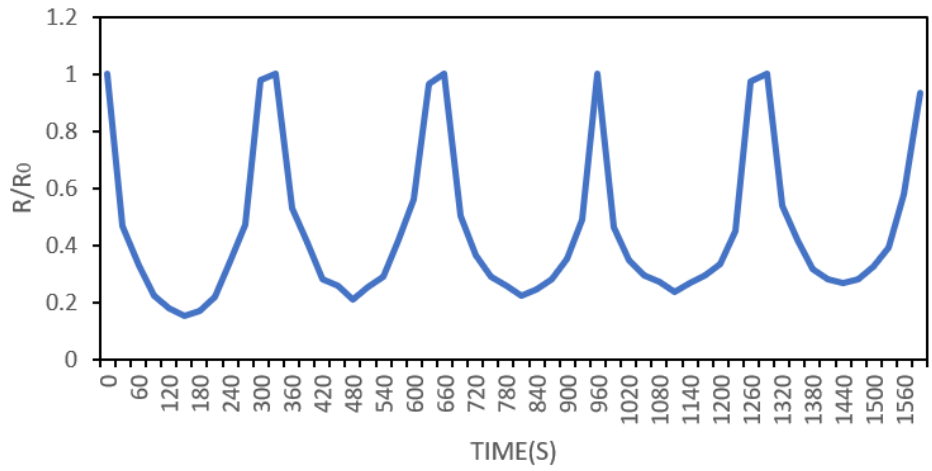

Figure 4-9 Piezoresistivity response of Nickel-PDMS under minor-pressure compressive strain cyclic test.

The pressure of one single weight was calculated as:

$$P = \frac{m \times g}{A} = \frac{0.045\ kg \times 9.8 \frac{m}{s^2}}{0.00693\ m^2} \approx 64\ Pa \quad (17)$$

where m is the weight, g the gravity constant and A the area of composite sheet.

Hence, we can calculate the maximum pressure over the composite was 320 Pa. With this amount of pressure, the electrical resistance of Nickel-PDMS composite dropped almost 80% with a repeatable accuracy especially after the first cycle. This extraordinary capability of this composite to capture minor stress as low as hundreds of pascals inspire us to explore areas where sensors with high sensitivity and accuracy are expected including human health monitoring and movement detection.

CHAPTER 5: Conclusion and Future Work

5.1 Research Conclusions

Effective and inexpensive fabrication method of flexible and stretchable piezo-resistive composite was studied and improved, the experiment results of each sample was listed below in Table 5.1. Compared to improvement in composite thickness, even spreading of conductive filler shows more significance in product performance. Conductive fillers including graphite and nickel were used with polydimethylsiloxane polymer matrix at an appropriate concentration, experiment result suggests that 35% Graphite-PDMS composite and 83% Nickel-PDMS composite exhibit the best piezoresistive performance and mechanical properties. Electrical resistance data obtained from experiment demonstrated excellent piezoresistivity performance under tensile and compressive strains, with minor compressive strain (<10%) our composite showed gauge factor of 10 and over 2 orders of resistance change were observed at moderate strain change (around 28%). Cyclic tests were conducted to further assess the repeatability of the composites, finding that the produced composites exhibit better repeatability and sensitivity in cyclic uniaxial compressive tests than tensile tests due to limited elasticity. However, the composites show different piezoresistive characterization in static and cyclic situations which may require further attention. Compared with market-available commercial piezoresistive sheet, our produced material usually has higher sensitivity but with narrower effective range (0 to 28%). Our composite also showed distinct piezoresistive response to external pressure as low as hundreds of Pascals with great repeatability. The overall performance of both Graphite-PDMS and Nickel-PDMS composites indicate vast prospect of application in minor-to-moderate strain sensor that demand high sensitivity and repeatability. With the development of advanced

manufacturing technology, this new piezoresistive composites can be of great use in human-health monitoring and industrial robot arm designs.

Table 5-1 Summarizes the piezoresistive response to tensile/compressive strain of each sample fabricated in experiment

Sample	Powder Size (μm)	Concentration (%)	Spincoat Settings (RPM*s)	Sample Thickness (inch)	Tensile Test Results	Compressive Test Results
GS1	3	35	1200 × 60	0.006	Showed poor elasticity at tensile strain and no meaningful results	Demonstrated 6 orders of gauge factor at 0.28 strain
GS2	3	40	1200 × 45	0.004		Demonstrated 1 order of gauge factor at 0.28 strain
GS3	25	40	1200 × 45	0.009		Showed 50% of resistance change at 0.28 strain change
GS4	25	40	1200 × 60	0.006		Demonstrated 2 orders of gauge factor at 0.28 strain

Table 5-1 (Continued)

GS5	25	40	800 × 45	0.009	Showed poor elasticity at tensile strain and no meaningful results	Showed unstable piezoresistive response under strain
GS6	25	40	800 × 60	0.008		
NS1	10	50	600 × 45	0.006	Showed no piezoresistive response to strain change	
NS2	10	83.3	600 × 30	0.025	Showed similar patterns of piezoresistivity and good consistency at early stage of tensile strain	Showed similar and obvious piezoresistive response to external compressive strain
NS3	10	83.3	600 × 45	0.017		
NS4	10	83.3	600 × 60	0.012		

5.2 Recommendation for Future Work

- More effective methods of mixing should be introduced to the fabrication process due to its large influence on final performance. Currently limited by the mixing capacity, certain concentrations of conductive filler cannot be fully tested due to uneven spreading and

tiny gap between conductive particles. However, composites with better piezoresistivity performance could be requiring such conditions.

- The effect of fabrication parameters should be further considered for design of experiment and their respective influence on piezoresistive responses. Experiments in this research is based on the fact that very limited knowledge of the influence of each parameter in composite fabrication, including conductive filler concentration and spincoat settings, were understood when the experiments began. Hence, the exploratory experiment performed in this study does not incorporate a comprehensive analysis of each parameter and the respective influence on the experimental results. With the preliminary results obtained from this study, we should focus on specific comparisons and optimizations in the future experiment design and analyses of the achieved experimental data with corresponding statistic studies.
- Composites fabricated in this research failed to demonstrate excellent elasticity with varying experiment parameters. However, in further applications of certain industrial area, including wearable device and human health monitoring, this might be an important requirement and takes up a large percentage of final assessment and decision. Future studies should focus on improvement of composite elasticity with new materials or fabricating methods to address this issue.
- Influence of environment should be studied. Environmental parameters including temperature and humidity could affect piezoresistivity performance and flexibility/stretchability according to previous research. However, those were not considered in this study by far since our experiments were all conducted under stable laboratory conditions with constant temperature and humidity parameters. Yet in

commercial applications, different usage scenarios are expected and we should not ignore the influence of this aspect.

- Piezoresistivity difference in static situation and cyclic process should be further investigated. Even though the performance remains stable after entering the cycles, discrepancy was observed when cyclic tests first start and this issue is surprisingly common in our various tests. Adjustment to composite structures or working parameter predictions should be done to better foresee the piezoresistive pattern and avoid excessive strain.
- Fatigue test with large repetition number should be done to examine whether life span of composites take a toll on product performance. Due to experimental limitations, large number of repetitions were not fulfilled. Other studies indicate that repetitions up to 1000 or 10000 times may cause wear and heat issues which will severely damage the piezoresistive performance and expected life span of sensors.

REFERENCES

[1] Chou, H., Nguyen, A., Chortos, A. *et al.* A chameleon-inspired stretchable electronic skin with interactive colour changing controlled by tactile sensing. *Nat Commun* 6**,** 8011 (2015).

[2] Y. Wu *et al*., "High resolution flexible strain sensors for biological signal measurements," *2017 19th International Conference on Solid-State Sensors, Actuators and Microsystems (TRANSDUCERS)*, Kaohsiung, 2017, pp. 1144-1147.

[3] Wu, Shuying & Peng, Shuhua & Wang, Chun-Hui. (2018). Stretchable strain sensors based on PDMS composites with cellulose sponges containing one- and two-dimensional nanocarbons. Sensors and Actuators A: Physical. 279. 10.1016/j.sna.2018.06.002.

[4] Chen, L.; Lu, L.; Wu, D.J.; Chen, G.H. Silicone rubber/graphite nanosheet electrically conducting nanocomposite with a low percolation threshold. Polym. Compos. 2007, 28, 493–498.

[5] Al-solamy, F.R., Al-Ghamdi, A.A. and Mahmoud, W.E. (2012), Piezoresistive behavior of graphite nanoplatelets based rubber nanocomposites. Polym. Adv. Technol., 23: 478-482. doi:10.1002/pat.1902

[6] Wu, Y., Karakurt, I., Beker, L., Kubota, Y., Xu, R., Ho, K.Y., Zhao, S., Zhong, J., Zhang, M., Wang, X., & Lin, L. (2018). Piezoresistive stretchable strain sensors with human machine interface demonstrations.

[7] Zhao, Hang & Bai, Jinbo. (2015). Highly Sensitive Piezo-Resistive Graphite Nanoplatelet–Carbon Nanotube Hybrids/Polydimethylsilicone Composites with Improved Conductive Network Construction. ACS applied materials & interfaces. 7. 10.1021/acsami.5b01413.

[8] Canavese, Giancarlo & Stassi, Stefano & Stralla, M. & Bignardi, Cristina & Pirri, C.F.. (2012). Stretchable and conformable metal–polymer piezoresistive hybrid system. Sensors and Actuators A: Physical. 186. 191-197. 10.1016/j.sna.2012.01.037.

[9] Jung, Joonhoo & Kim, Minjae & Choi, Jin & Park, Dong-Wha & Shim, Sang. (2013). Piezoresistive effects of copper-filled polydimethylsiloxane composites near critical pressure. Polymer. 54. 10.1016/j.polymer.2013.11.012.

[10] Meskinis, Sarunas & Gudaitis, R & Vasiliauskas, A & Čiegis, A & Šlapikas, K & Tamulevičius, T & Andrulevičius, Mindaugas & Tamulevičius, Sigitas. (2015). Piezoresistive properties of diamond like carbon films containing copper. Diamond and Related Materials. vol.60. p. 20- 25. 10.1016/j.diamond.2015.10.007.

[11] Stassi, Stefano & Canavese, Giancarlo & Cosiansi, Fernando & Gazia, R & Cocuzza, Matteo. (2013). A Tactile Sensor Device Exploiting the Tunable Sensitivity of Copper-PDMS Piezoresistive Composite. Procedia Engineering. 47. 10.1016/j.proeng.2012.09.233.

[12] He, Y., Li, W., Yang, G., Liu, H., Lu, J., Zheng, T., & Li, X. (2017). A Novel Method for Fabricating Wearable, Piezoresistive, and Pressure Sensors Based on Modified-Graphite/Polyurethane Composite Films. *Materials (Basel, Switzerland)*, *10*(7), 684. https://doi.org/10.3390/ma10070684

[13] Johnson, Oliver & Gardner, Calvin & Fullwood, David & Adams, Brent & Hansen, Nathan & Hansen, George. (2010). The Colossal Piezoresistive Effect in Nickel Nanostrand Polymer Composites and a Quantum Tunneling Model. Computers, Materials and Continua. 15. 87-111. 10.4135/9781483349398.n5.

[14] Stassi, Stefano & Canavese, Giancarlo & Valentina, Cauda & Marasso, Simone & Pirri, Candido. (2012). Evaluation of different conductive nanostructured particles as filler in

smart piezoresistive composites. Nanoscale research letters. 7. 327. 10.1186/1556-276X-7-327.

[15] Abyaneh, Majid & Ekar, Satish & Kulkarni, Sulabha. (2012). Piezoresistivity and Mechanical Behavior of Metal-polymer Composites under Uniaxial Pressure. J. Mater. Sci. Res.. 1. 10.5539/jmsr.v1n3p50.

[16] Lu, Jingrong & Chen, Xiangfeng & Lu, Wei & Chen, Guohua. (2006). The piezoresistive behaviors of polyethylene/foliated graphite nanocomposites. European Polymer Journal - EUR POLYM J. 42. 1015-1021. 10.1016/j.eurpolymj.2005.11.026.

[17] Zhu, Shou-En & Ghatkesar, Murali & Zhang, Chao & Janssen, G.. (2013). Graphene Based Piezoresistive Pressure Sensor. Applied Physics Letters. 102. 10.1063/1.4802799.

[18] Wang, Yunming & Mi, Hongyi & Zheng, Qifeng & Zhang, Huilong & Ma, Zhenqiang & Gong, Shaoqin. (2015). Highly Stretchable and Sensitive Piezoresistive Carbon Nanotube /Elastic Triisocyanate-Crosslinked Polytetrahydrofuran Nanocomposites. J. Mater. Chem. C. 4. 10.1039/C5TC03413B.

[19] Ke, Kai & Pötschke, Petra & Wiegand, Niclas & Krause, Beate & Voit, Brigitte. (2016). Tuning the Network Structure in Poly(vinylidene fluoride)/Carbon Nanotube Nanocomposites Using Carbon Black: Toward Improvements of Conductivity and Piezoresistive Sensitivity. ACS Applied Materials & Interfaces. 8. 10.1021/acsami.6b03451.

[20] Nag, Anindya & Afsarimanesh, Nasrin & Feng, Shilun & Mukhopadhyay, S.C.. (2018). Strain induced graphite/PDMS sensors for biomedical applications. Sensors and Actuators A Physical. 271. 10.1016/j.sna.2018.01.044.

[21] Aravamudhan, Shyam & Bhansali, Shekhar. (2008). Reinforced piezoresistive pressure sensor for ocean depth measurements. Sensors and Actuators A: Physical. 142. 111-117. 10.1016/j.sna.2007.04.036.

[22] S. Samaun, K. Wise, E. Nielsen and J. Angell, "An IC piezoresistive pressure sensor for biomedical instrumentation," 1971 IEEE International Solid-State Circuits Conference. Digest of Technical Papers, Philadelphia, PA, USA, 1971, pp. 104-105.

[23] Alamusi, Hu, N., Fukunaga, H., Atobe, S., Liu, Y., & Li, J. (2011). Piezoresistive Strain Sensors Made from Carbon Nanotubes Based Polymer Nanocomposites. *Sensors*.

[24] Zhao H, Zhang Y, Bradford PD, Zhou Q, Jia Q, Yuan F et al. Carbon nanotube yarn strain sensors. Nanotechnology 2010;21:305502.

[25] J. D. BERNAL, Proc. Roy. Soc. A106 (1924) 749

[26] R. W. G. WYCKOFF , “Crystal Structures,” Vol. 1 (Interscience, New York, 1963).

[27] Feng, Chang & Ni, Haiying & Chen, Jun & Yang, Wei. (2016). Facile Method to Fabricate Highly Thermally Conductive Graphite/PP Composite with Network Structures. ACS applied materials & interfaces. 8. 10.1021/acsami.6b03723.

[28] Sun, Jie & Zheng, Guangyuan & Lee, Hyun-Wook & Liu, Nian & Wang, Haotian & Yao, Hongbin & Yang, Wensheng & Cui, Yi. (2014). Formation of Stable Phosphorus-Carbon Bond for Enhanced Performance in Black Phosphorus Nanoparticle-Graphite Composite Battery Anodes. Nano Letters. 14. 4573-4580. 10.1021/nl501617j.

[29] Motozuka, Satoshi & Tagaya, M. & Ikoma, Toshiyuki & Yoshioka, Tomohiko & Xu, Z.F. & Tanaka, J.. (2012). Preparation of copper-graphite composite particles by milling process. Journal of Composite Materials. 46. 2829-2834. 10.1177/0021998311432947.

[30] National Pollutant Inventory – Nickel and compounds Fact SheetArchived December 8, 2011, at the Wayback Machine. Npi.gov.au. Retrieved on January 9, 2012.

[31] Rosenberg, Samuel J. (1968). Nickel and Its Alloys. National Bureau of Standards.

[32] McNeil, Ian (1990). "The Emergence of Nickel". An Encyclopaedia of the History of Technology. Taylor & Francis. pp. 96–100. ISBN 978-0-415-01306-2.

[33] Chen, Xu & Cheng, F. & Li, S. & Zhou, Lingping & Li, Dai-Yin. (2002). Electrodepo Sited Nickel Composites Containing Carbon Nanotubes. Surface & Coatings Technology - SURF COAT TECH. 155. 274-278. 10.1016/S0257-8972(02)00118-4.

[34] Kuang, Da & Xu, Liye & Lei, Liu & Hu, Wenbin & Wu, Yating. (2013). Graphene–nickel composites. Applied Surface Science. 273. 484–490. 10.1016/j.apsusc.2013.02.066.

[35] Tench, D., White, J. Enhanced tensile strength for electrodeposited nickel-copper multilayer composites. MTA 15, 2039–2040 (1984).

[36] Gonsalves, Kenneth & Merhari, L. & wu, Hengpeng & Hu, YQ. (2001). Organic–Inorganic Nanocomposites: Unique Resists for Nanolithography. Advanced Materials. 13. 703 - 714. 10.1002/1521-4095(200105)13:10<703::AID-ADMA703>3.0.CO;2-A.

[37] Sia, Samuel & Whitesides, George. (2003). Microfluidic Devices Fabricated in Poly(Dimethylsiloxane) for Biological Studies. Electrophoresis. 24. 3563-76. 10.1002/elps.200305584.

[38] Rogers, John & Nuzzo, Ralph. (2005). Recent progress in soft lithography. Materials Today. 8. 50-56. 10.1016/S1369-7021(05)00702-9.

[39] Hoang, Michelle & Chung, Hyun-joong & Elias, Anastasia. (2016). Irreversible bonding of polyimide and polydimethylsiloxane (PDMS) based on a thiol-epoxy click reaction. Journal of Micromechanics and Microengineering. 26. 10.1088/0960-1317/26/10/105019.

[40] Lee, Hanleem & Lee, Keunsik & Park, Jin & Kim, Woon & Lee, Hyoyoung. (2014). Well-Ordered and High Density Coordination-Type Bonding to Strengthen Contact of Silver Nanowires on Highly Stretchable Polydimethylsiloxane. Advanced Functional Materials. 24. 10.1002/adfm.201303276.

[41] Lin, Chien-Hong & Yeh, Yi-Hsing & Lin, Wen-Ching & Yang, Ming-Chien. (2014). Novel silicone hydrogel based on PDMS and PEGMA for contact lens application. Colloids and Surfaces B: Biointerfaces. 123. 10.1016/j.colsurfb.2014.10.053.

[42] B. J. Basu, T. Bharathidasan and C. Anandan, Surf. Innovations, 2013, 1, 40.

[43] Burgess, Ian. (2009). The mode of action of dimeticone 4% lotion against head lice, Pediculus captis. BMC pharmacology. 9. 3. 10.1186/1471-2210-9-3.

[44] Tottey, Leah & Coulson, Sally & Wevers, Gerhard & Fabian, Laura & McClelland, Heather & Dustin, Mickayla. (2018). Persistence of Polydimethylsiloxane Condom Lubricants. Journal of Forensic Sciences. 64. 10.1111/1556-4029.13816.

[45] Dong, Niu & Jiang, Weitao & Ye, Guoyong & Wang, Kun & Yin, Lei & Shi, Yongsheng & Chen, Bangdao & Luo, Feng & Liu, Hongzhong. (2018). Graphene-elastomer nanocomposites based flexible piezoresistive sensors for strain and pressure detection. Materials Research Bulletin. 102. 10.1016/j.materresbull.2018.02.005.

[46] Thomson W. On the electro-dynamic qualities of metals: Effects of magnetization on the electric conductivity of nickel and of iron. Proc R Soc Lond 1856;8:546-550.

[47] Barlian, A.A.; Park, W.-T.; Mallon, J.R.; Rastegar, A.J.; Pruitt, B.L. (March 2009). "Review: Semiconductor Piezoresistance for Microsystems". Proceedings of the IEEE. 97 (3): 513–552. doi:10.1109/jproc.2009.2013612. ISSN 0018-9219. PMC 2829857. PMID 20198118.

[48] Sun Y. Strain effect in semiconductors: theory and device applications. New York: Springer Dec. 2009, 2009.

[49] Smith CS. Piezoresistance effect in germanium and silicon. Physical Review 1954;94:42-9.

[50] Harsányi G. Sensors in biomedical applications : fundamentals, technology & applications. Lancaster, Pa.: Technomic Pub Co, 2000.

[51] Zheng Q, Zhou JF, Song YH. Time-dependent uniaxial piezoresistive behavior of highdensity polyethylene/short carbon fiber conductive composites. J Mater Res 2004;19:2625-

[52] Lu JR, Weng WG, Chen XF, Wu DJ, Wu CL, Chen GH. Piezoresistive materials from directed shear-induced assembly of graphite nanosheets in polyethylene. Adv Funct Mater 2005;15:1358-63.

[53] Boschetti-de-Fierro A, Pardey R, Savino V, Mueller AJ. Piezoresistive behavior of epoxy matrix-carbon fiber composites with different reinforcement arrangements. J Appl Polym Sci 2009;111:2851-8.

[54] Yan, Chaoyi & Wang, Jiangxin & Kang, Wenbin & Cui, Mengqi & Wang, Xu & Foo, Ce Yao & Kenji, Chee & Lee, Pooi See. (2014). Highly Stretchable Piezoresistive Graphene–Nanocellulose Nanopaper for Strain Sensors. Advanced Materials. 26. 10.1002/adma.201304742.

[55] Luo, Ningqi & Dai, Wenxuan & Chenglin, Li & Zhou, Zhiqiang & Lu, Liyuan & Poon, Carmen & Chen, Shih-Chi & Zhang, Yuan-Ting & Zhao, Ni. (2015). Flexible Piezoresistive Sensor Patch Enabling Ultralow Power Cuffless Blood Pressure Measurement. Advanced Functional Materials. 26. 10.1002/adfm.201504560.

[56] Liu, Xinyu & Mwangi Thuo, Martin & Li, Xiujun & O'Brien, Michael & Whitesides, George. (2011). Paper-based piezoresistive MEMS sensors. Lab on a chip. 11. 2189-96. 10.1039/c1lc20161a.

[57] Chen, Ling & Chen, G. H & Lu, Liang. (2007). Piezoresistive Behavior Study on Finger-Sensing Silicone Rubber/Graphite Nanosheet Nanocomposites. Advanced Functional Materials. 17. 898 - 904. 10.1002/adfm.200600519.

APPENDICES

Appendix A

As a supplement of the thesis, some results obtained from initial trial experiments that are not significant enough (the experimental results that failed to exhibit stable and consistent patterns or meaningful responses) to present and discuss in main body are displayed here. With the help of such data, further experiment can be conducted with better precision.

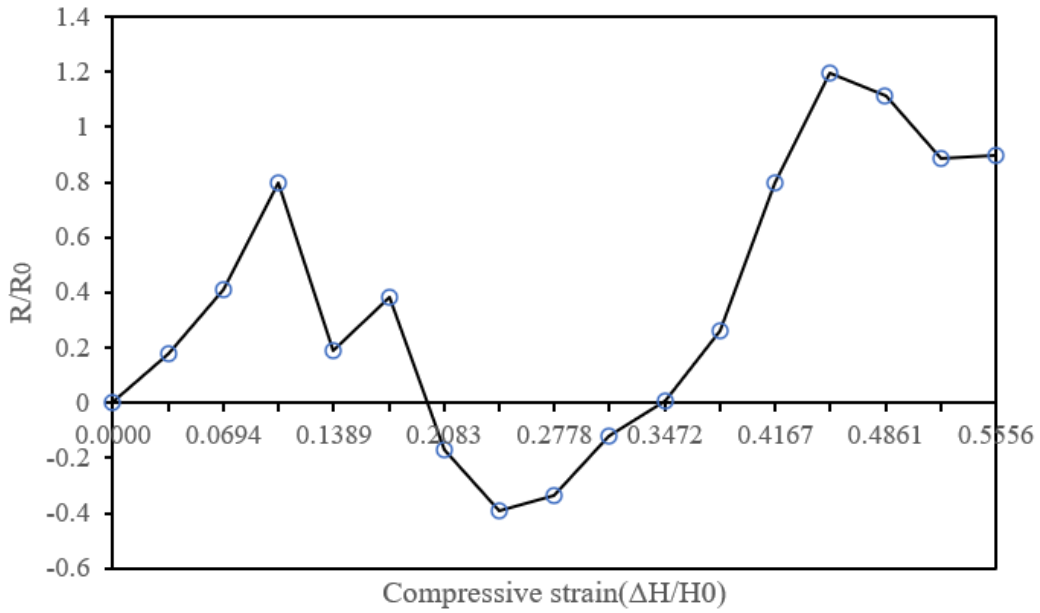

Figure A1 Uniaxial compressive strain test result of 40% weight ratio Graphite-PDMS composite with 800 rpm * 45 s spincoating.

The uniaxial compressive strain test result of sample GS5 is shown above as Figure A1. As the figure suggests, the result fluctuates heavily (from -40% to 20%) throughout the compressive strain range and fails to demonstrate clear response patterns. Besides from the averaged value shown in the figure, the actual data recorded in the experiment also fluctuates in a large range

and causes a large variance for the averaged value. Hence we believe that the result obtained in this experiment should be omitted in main body and more experiments are needed in future studies to observe the reasons of this unstable result and respective solutions to that.

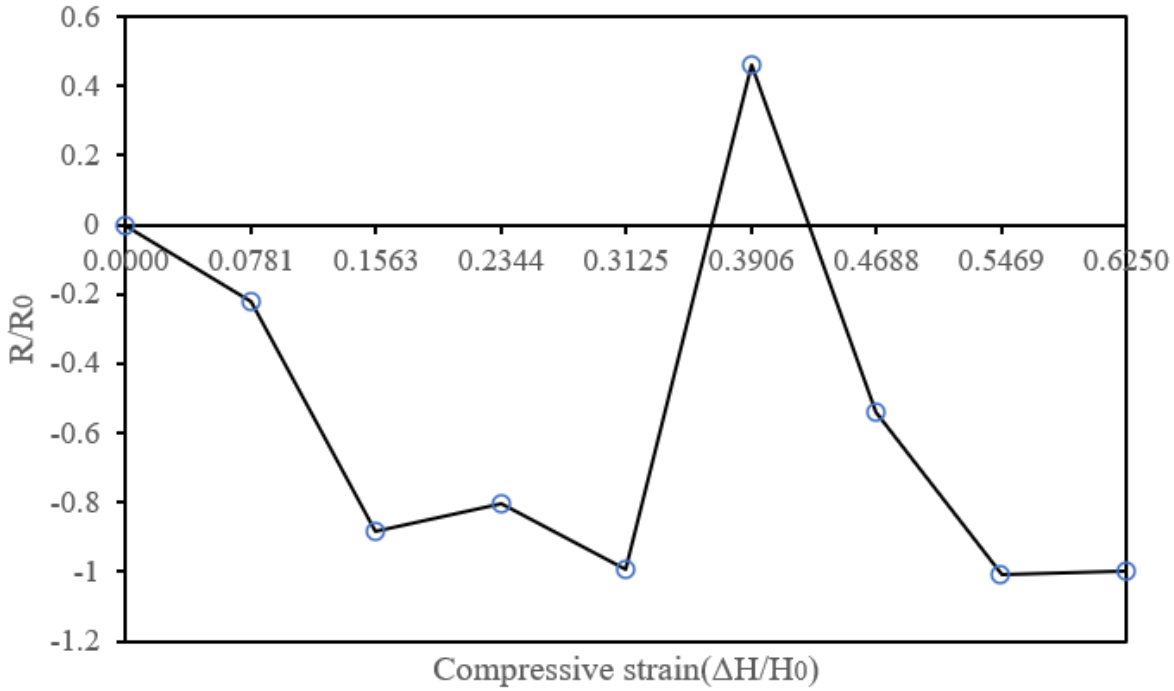

Figure A2 Uniaxial compressive strain test result of 40% weight ratio Graphite-PDMS composite with 800 rpm * 60 s spincoating test data 1.

The reason for us to omit the uniaxial compressive strain test result 1 of sample GS6 is similar to that of GS5 which was discussed above.

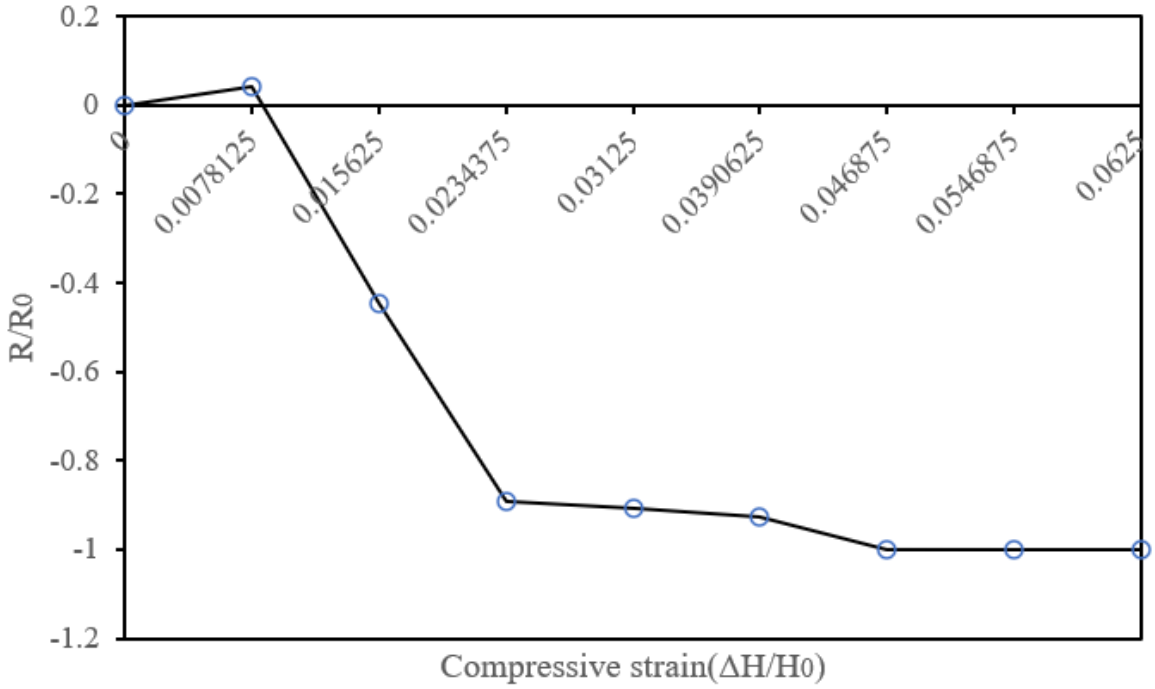

Figure A3 Uniaxial compressive strain test result of 40% weight ratio Graphite-PDMS composite with 800 rpm * 60 s spincoating test data 2.

The second set of uniaxial compressive strain test result of sample GS6 is shown above as Figure A3. Because of the unstable result we obtained from the first test, we conducted a second GS6 compressive strain test to figure out whether this was a test error. From the figure above we can find that the piezoresistive response pattern of GS6 in this test does show gradually declining trend which is similar to results from other Graphite-PDMS samples. However, the actual data recorded from experiments still showed a large variance. Hence consider the contradicted results we obtained from two sets of experiment, we decided to omit the uniaxial compressive strain result of sample GS6 until further tests are conducted and clear conclusion was made.

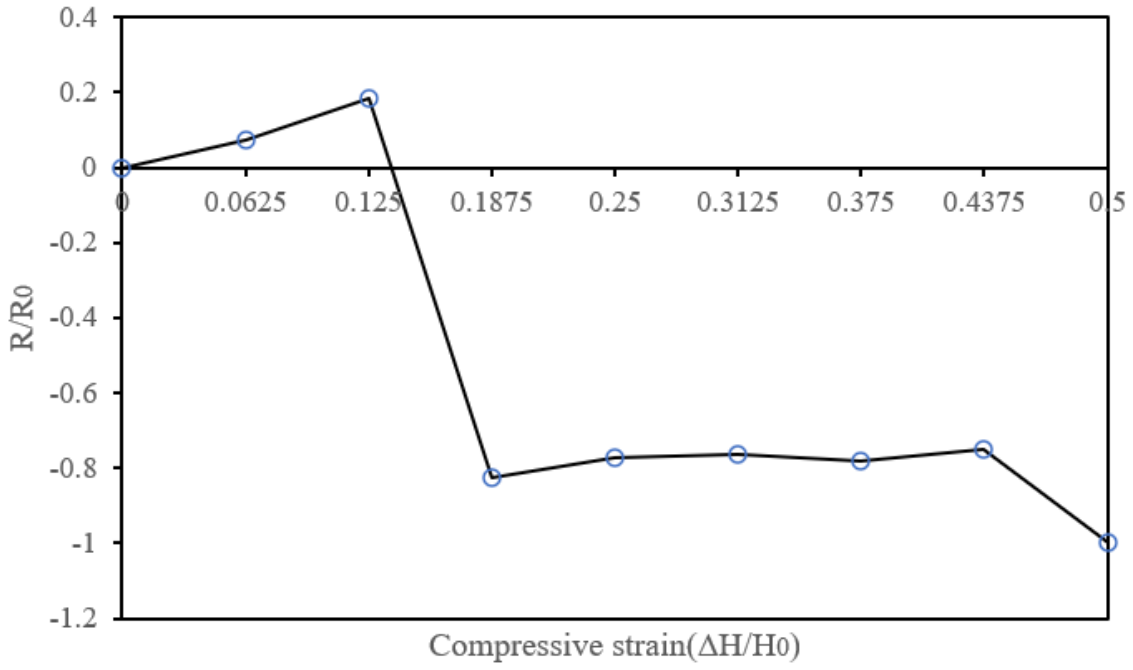

Figure A4 Uniaxial compressive strain test result of 40% weight ratio Graphite-PDMS composite with 1200 rpm * 45 s spincoating.

Figure A4 shows the uniaxial compressive strain test result of sample GS2. As the result shows, sample GS2 demonstrates a generally declining trend in electrical resistance as external compressive strain increases. However, compared to other Graphite-PDMS samples, the piezoresistive responses to moderate compressive strain (around 25% strain change) is lower. GS2 demonstrates only 80% of resistance change at 20% compressive strain and from 20% to 45% strain change the resistance remains stable (less than 10% resistance change). Hence, we consider the sensitivity to compressive strain of sample GS2 is lower than other graphite-PDMS samples and left the result of it out of results discussion part.